



**HAL**  
open science

***Rhodobacter sphaeroides* methionine sulfoxide reductase P reduces *R* - and *S* -diastereomers of methionine sulfoxide from a broad-spectrum of protein substrates**

Lionel Tarrago, Sandrine Grosse, Marina I. Siponen, David Lemaire, Béatrice Alonso, Guylaine Miotello, J. Armengaud, Pascal Arnoux, David Pignol, Monique Sabaty

► **To cite this version:**

Lionel Tarrago, Sandrine Grosse, Marina I. Siponen, David Lemaire, Béatrice Alonso, et al.. *Rhodobacter sphaeroides* methionine sulfoxide reductase P reduces *R* - and *S* -diastereomers of methionine sulfoxide from a broad-spectrum of protein substrates. *Biochemical Journal*, 2018, 475 (23), pp.3779-3795. 10.1042/BCJ20180706 . cea-01936753

**HAL Id: cea-01936753**

**<https://cea.hal.science/cea-01936753>**

Submitted on 13 Dec 2018

**HAL** is a multi-disciplinary open access archive for the deposit and dissemination of scientific research documents, whether they are published or not. The documents may come from teaching and research institutions in France or abroad, or from public or private research centers.

L'archive ouverte pluridisciplinaire **HAL**, est destinée au dépôt et à la diffusion de documents scientifiques de niveau recherche, publiés ou non, émanant des établissements d'enseignement et de recherche français ou étrangers, des laboratoires publics ou privés.

1 ***Rhodobacter sphaeroides* methionine sulfoxide reductase P reduces *R*- and *S*-diastereomers of**  
2 **methionine sulfoxide from a broad-spectrum of protein substrates**

3 Lionel Tarrago<sup>1,\*</sup>, Sandrine Grosse<sup>1</sup>, Marina I. Siponen<sup>1</sup>, David Lemaire<sup>2</sup>, Béatrice Alonso<sup>1</sup>, Guylaine  
4 Miotello<sup>3</sup>, Jean Armengaud<sup>3</sup>, Pascal Arnoux<sup>1</sup>, David Pignol<sup>1</sup>, Monique Sabaty<sup>1,\*</sup>

5 <sup>1</sup>Aix Marseille Univ, CEA, CNRS, BIAM, Laboratoire de bioénergétique cellulaire, Saint  
6 Paul-Lez-Durance, France F-13108; <sup>2</sup>Aix Marseille Univ, CEA, CNRS, BIAM, Laboratoire des Interactions  
7 Protéine-Métal, Saint Paul-Lez-Durance, France F-13108; <sup>3</sup>Laboratoire Innovations technologiques pour la  
8 Détection et le Diagnostic (Li2D), Service de Pharmacologie et Immunoanalyse (SPI), CEA, INRA,  
9 F-30207 Bagnols sur Cèze, France.

10

11 \*Correspondence: Lionel Tarrago ([lioneltarrago@msn.com](mailto:lioneltarrago@msn.com)) or Monique Sabaty ([monique.sabaty@cea.fr](mailto:monique.sabaty@cea.fr))

12

13

14 **Keywords:** Enzyme kinetics, methionine sulfoxide reductase, microbiology, molybdoenzyme, oxidative  
15 stress, periplasm, protein oxidation, proteomics

16 **Abstract**

17 Methionine (Met) is prone to oxidation and can be converted to Met sulfoxide (MetO), which exists as  
18 *R*- and *S*-diastereomers. MetO can be reduced back to Met by the ubiquitous methionine sulfoxide reductase  
19 (Msr) enzymes. Canonical MsrA and MsrB were shown to be absolutely stereospecific for the reduction of  
20 *S*- and *R*-diastereomer, respectively. Recently, a new enzymatic system, MsrQ/MsrP which is conserved in  
21 all gram-negative bacteria, was identified as a key actor in the reduction of oxidized periplasmic proteins.  
22 The haem-binding membrane protein MsrQ transmits reducing power from the electron transport chains to  
23 the molybdoenzyme MsrP, which acts as a protein-MetO reductase. The MsrQ/MsrP function was well  
24 established genetically, but the identity and biochemical properties of MsrP substrates remain unknown. In  
25 this work, using the purified MsrP enzyme from the photosynthetic bacteria *Rhodobacter sphaeroides* as a  
26 model, we show that it can reduce a broad spectrum of protein substrates. The most efficiently reduced  
27 MetO are found in clusters of amino acid sequences devoid of threonine and proline on the C-terminal side.  
28 Moreover, *R. sphaeroides* MsrP lacks stereospecificity as it can reduce both *R*- and *S*- diastereomers of  
29 MetO, similarly to its *Escherichia coli* homolog, and preferentially acts on unfolded oxidized proteins.  
30 Overall, these results provide important insights into the function of a bacterial envelop protecting system,  
31 which should help understand how bacteria cope in harmful environments.

32

33 **Abbreviations:** BV, benzyl viologen; DMSO, dimethylsulfoxide; DTT, dithiothreitol; ESI-MS,  
34 Electrospray Ionization-Mass spectrometry; H<sub>2</sub>O<sub>2</sub>, hydrogen peroxide;  
35 HEPES4-(2-hydroxyethyl)-1-piperazineethanesulfonic acid; MES, 2-(N-morpholino)ethanesulfonic acid;  
36 MetO, methionine sulfoxide; Met-*R*-O, *R*-diastereomer of MetO; Met-*S*-O, *S*-diastereomer of MetO; MS,  
37 mass spectrometry, Msr, MetO reductase, NADPH, Nicotinamide adenine dinucleotide phosphate; NaOCl,  
38 sodium hypochlorite.

## 39 **Introduction**

40 Aerobic life exposes organisms to reactive oxygen species (ROS) derived from molecular oxygen, such  
41 as hydrogen peroxide (H<sub>2</sub>O<sub>2</sub>) or singlet oxygen (<sup>1</sup>O<sub>2</sub>). Bioenergetic chains are important sources of these  
42 intracellular ROS. H<sub>2</sub>O<sub>2</sub> is principally produced during respiration [1] and <sup>1</sup>O<sub>2</sub> arises from photosynthesis  
43 [2]. In most organisms, these oxidative molecules act as signaling messengers playing major roles in  
44 numerous physiological and pathological states. Furthermore, their production and elimination are tightly  
45 regulated [3]. However, numerous stresses can affect ROS homeostasis and increase their intracellular  
46 concentration to excessive values leading to uncontrolled reactions with sensitive macromolecules [4]. For  
47 instance, photosynthetic organisms, such as plants or the purple bacteria *Rhodobacter sphaeroides* can  
48 experience photo-oxidative stress in which unbalance between incident photons and photosynthetic electron  
49 transfer generate detrimental accumulation of <sup>1</sup>O<sub>2</sub> [5]. Moreover, production of ROS could be used  
50 advantageously in a defensive strategy against potential pathogenic invaders. For instance, neutrophils  
51 produce the strong oxidant hypochlorite (ClO<sup>-</sup>) from H<sub>2</sub>O<sub>2</sub> and chlorine ions to eliminate bacteria and fungi  
52 [3]. Because of their abundance in cells, proteins are the main targets of oxidation [6]. Methionine (Met) is  
53 particularly prone to oxidation and the reaction of Met with an oxidant leads to the formation of Met  
54 sulfoxide (MetO), which exists as two diastereomers *R* (Met-*R*-O) and *S* (Met-*S*-O). Further oxidation can  
55 then lead to the formation of Met sulfone (MetO<sub>2</sub>) [7,8]. As opposed to most oxidative modifications on  
56 amino acids, the formation of MetO is reversible, and oxidized proteins can be repaired thanks to methionine  
57 sulfoxide reductases (Msr) enzymes that principally exist in two types, MsrA and MsrB. These enzymes,  
58 present in almost all organisms, did not evolve from a common ancestral gene and possess an absolute  
59 stereospecificity towards their substrates. Indeed, MsrA can reduce only Met-*S*-O [7,9–12] whereas MsrB  
60 acts only on Met-*R*-O [10–14]. This strict stereospecificity was enzymatically demonstrated using  
61 chemically prepared Met-*R*-O and Met-*S*-O from racemic mixtures of free MetO or by using HPLC methods  
62 allowing discrimination of both diastereomers. A structural explanation was also provided by deciphering  
63 the mirror images of their active sites, in which only one MetO diastereomer can be accommodated [10].

64 While MsrA can reduce Met-S-O, whether as a free amino acid or included in proteins, MsrB is specialized  
65 in the reduction of protein-bound Met-R-O, and both are more efficient on unfolded oxidized proteins  
66 [15,16]. Eukaryotic Msrs are important actors in oxidative stress protection, aging and neurodegenerative  
67 diseases in animals [17], during environmental stresses and seed longevity in plants [18,19]. In bacteria,  
68 MsrA and MsrB are generally located in the cytoplasm [3], except in *Neisseria* or *Streptococcus* species,  
69 for which MsrA and MsrB enzymes can be addressed to the envelope [20,21]. They play a role in protecting  
70 against oxidative stress and as virulence factors [3].

71 Beside these stereotypical Msrs found in all kinds of organisms, several other enzymes can catalyze  
72 MetO reduction, principally in bacteria. For instance, numerous bacteria as well as unicellular eukaryotes,  
73 such as *Saccharomyces cerevisiae*, possess another type of absolutely stereospecific Msr, called free-R-Msr  
74 (fRMsr) or MsrC, which is specialized in the reduction of the free form of Met-R-O [22,23]. As MsrA and  
75 MsrB, the fRMsr uses thiol-based chemistry and the reducing power coming from NADPH to reduce its  
76 substrate [22,23].

77 In bacteria, several molybdenum cofactor-containing enzymes were also shown to be able to reduce  
78 oxidized Met. Particularly, the biotin sulfoxide reductase BisC, or its homolog TorZ/BisZ, specifically  
79 reduce the free form of Met-S-O, in the *Escherichia coli* cytoplasm and the *Haemophilus influenza*  
80 periplasm, respectively [24,25]. Moreover, *E. coli* DMSO reductase reduces a broad spectrum of substrates,  
81 including MetO [26], while the *R. sphaeroides* homolog was shown to be absolutely stereospecific towards  
82 S-enantiomer of several alkyl aryl sulfoxides [27]. Finally, another molybdoenzyme, MsrP (formerly known  
83 as YedY), was recently identified as a key player of MetO reduction in the periplasm [28,29]. MsrP was  
84 shown to be induced by exposure to the strong oxidant hypochlorite (ClO<sup>-</sup>) and to reduce MetO on several  
85 abundantly present periplasmic proteins in *E. coli* [28] or on a Met-rich protein in *Azospira suillum* [29]. A  
86 most striking feature of *E. coli* MsrP (EcMsrP) is that, contrary to all known methionine sulfoxide  
87 reductases, it seems capable of reducing both Met-R-O and Met-S-O [28]. The cistron, *msrP*, belongs to an  
88 operon together with the cistron encoding the transmembrane protein MsrQ, which is responsible for the

89 electron transfer to MsrP from the respiratory chain. Of note, the cytosolic flavin reductase Fre was proposed  
90 as a potential alternative electron-carrier to MsrQ [30]. The operon is conserved in the genome of most  
91 gram-negative bacteria suggesting that the MsrP/Q system is very likely a key player for general protection  
92 in the bacterial envelop against deleterious protein oxidation [28,29]. *R. sphaeroides* MsrP (RsMsrP) shares  
93 50% of identical amino acid residues with EcMsrP and transcriptomic analyses evidenced that *RsmsrP* is  
94 strongly induced under high-light conditions, suggesting a putative role in protecting the periplasm against  
95  $^1\text{O}_2$  [31].

96 In this paper, we describe the biochemical characterization of RsMsrP regarding its substrate specificity.  
97 Using kinetic activity experiments and mass spectrometry analysis, we show that RsMsrP is a very efficient  
98 protein-bound MetO reductase, which lacks stereospecificity and preferentially acts on unfolded oxidized  
99 proteins. Proteomic analysis indicates that it can reduce a broad spectrum of proteins in the *R. sphaeroides*  
100 periplasm, and that Met sensitive to oxidation and efficiently reduced by RsMsrP are found in clusters and  
101 in specific amino acids sequences.

102

103 **Material and methods**

104 **Production and purification of recombinant proteins**

105 Recombinant MsrP was produced similarly to the previously described protocol [32]. Briefly, *R.*  
106 *sphaeroides* f sp. *denitrificans* IL106 *dmsA*<sup>-</sup> strain carrying the pSM189 plasmid for production of a  
107 periplasmic MsrP with a 6-His N-terminal tag was grown in 6-liter culture under semi-aerobic conditions  
108 in Hutner medium until late exponential phase. The periplasmic fraction was extracted and loaded on a  
109 HisTrap column (GE Healthcare), MsrP was then eluted by an imidazole step gradient. MsrP solution was  
110 concentrated using 15-ml Amicon<sup>®</sup> Ultra concentrators with 10-kDa cutoff (Millipore), desalted with  
111 Sephadex G-25 in PD-10 Desalting Columns (GE Healthcare). The protein concentration was adjusted to 1  
112 mg.ml<sup>-1</sup> in 30 mM Tris-HCl pH 7.5, 500 mM NaCl, the Tobacco Etch Virus (TEV) protease was added  
113 (1:80 TEV:RsMsrP mass ratio) and the solution incubated overnight at room temperature to remove the  
114 polyhistidine tag. Untagged RsMsrP was purified on a second HisTrap column, then concentrated and  
115 desalted in 50 mM 4-(2-hydroxyethyl)-1-piperazineethanesulfonic acid (HEPES) pH 8.0. Protein solution  
116 was then loaded on a Superdex<sup>™</sup> 200 10/30 gel filtration column equilibrated with 30 mM Tris-HCl pH  
117 7.5. Main fractions were pooled and applied to a MonoQ<sup>™</sup> 4.6/100 PE (GE Healthcare). RsMsrP was then  
118 eluted using a linear NaCl gradient (0 to 500 mM). Fractions were analyzed on SDS-PAGE using  
119 NuPAGE<sup>™</sup>, 10 % Bis-Tris gels with MES-SDS buffer (ThermoFisher). Recombinant MsrA, MsrB,  
120 Thioredoxin Reductase (TR) 1, Thioredoxin 1 (Trx1) from *Saccharomyces cerevisiae* with polyhistidine  
121 tags, as well as the glutathione-S-transferase (GST) from *Schistosoma japonicum*, were produced and  
122 purified as previously described [15]. Protein concentrations were determined spectrophotometrically using  
123 specific molar extinction coefficients at 280 nm: 6-His-RsMSRP, 56,380 M<sup>-1</sup>.cm<sup>-1</sup>; untagged RsMsrP,  
124 54,890 M<sup>-1</sup>.cm<sup>-1</sup>; MsrA, 34,630 M<sup>-1</sup>.cm<sup>-1</sup>; MsrB, 24,325 M<sup>-1</sup>.cm<sup>-1</sup>; TR1, 24,410 M<sup>-1</sup>.cm<sup>-1</sup>; Trx1, 9,970  
125 M<sup>-1</sup>.cm<sup>-1</sup>; GST, 42,860 M<sup>-1</sup>.cm<sup>-1</sup>, bovine β-casein (Sigma-Aldrich), 11,460 M<sup>-1</sup>.cm<sup>-1</sup> and chicken lysozyme  
126 (Sigma-Aldrich), 32,300 M<sup>-1</sup>.cm<sup>-1</sup>. Protein solutions were stored at -20°C until further use.

127

128 **Peptides**

129 Ser-Met(O)-Ser, QWGAGM(O)QAEED and TTPGYM(O)EEWNK peptides were obtained from  
130 GenScript® (Hong-Kong).

131 **Preparation of oxidized bovine  $\beta$ -casein and its Met-R-O and Met-S-O containing counterparts**

132 For oxidation, bovine  $\beta$ -casein was prepared in Phosphate Buffered Saline (PBS) at 1 mg.ml<sup>-1</sup> in the  
133 presence of 200 mM H<sub>2</sub>O<sub>2</sub> and incubated overnight at room temperature. H<sub>2</sub>O<sub>2</sub> was removed by desalting  
134 using a PD-10 column and the protein solution was concentrated with 10-kDa cutoff Amicon® Ultra  
135 concentrator. Oxidized GST was similarly prepared using 100 mM H<sub>2</sub>O<sub>2</sub>. To prepare Met-R-O containing  
136  $\beta$ -casein, a solution of oxidized  $\beta$ -casein was incubated in 30 mM Tris-HCl pH 8 at a final concentration of  
137 6.5 mg.ml<sup>-1</sup> (260  $\mu$ M) in the presence of 25 mM dithiothreitol (DTT) with 10  $\mu$ M MsrA and incubated  
138 overnight at room temperature. The solution was diluted 10-fold in 30 mM Tris-HCl pH 8 and passed over  
139 a HisTrap column to remove the his-tagged MsrA. After concentration, the DTT was removed by desalting  
140 using a PD-10 column. Met-S-O containing  $\beta$ -casein was prepared similarly replacing the MsrA by the  
141 MsrB (14  $\mu$ M). The protein solutions were concentrated with a 10-kDa cutoff Amicon® Ultra concentrator  
142 and the final concentration was determined spectrophotometrically. Protein solutions were stored at -20°C  
143 until further use.

144 **Enzymatic activity and apparent stoichiometry measurements**

145 RsMsrP reductase activity was measured as described in ref. [32] with a few modifications. Benzyl  
146 viologen (BV) was used as an electron donor and its consumption was followed at 600 nm using an UVmc1®  
147 spectrophotometer (SAFAS Monaco) equipped with optic fibers in a glovebox workstation (MBRAUN  
148 Labstar) flushed with nitrogen. We determined the specific molar extinction coefficient of benzyl viologen  
149 at 8,700 M<sup>-1</sup>.cm<sup>-1</sup> in 50 mM 2-(*N*-morpholino)ethanesulfonic acid (MES), pH 6.0 buffer. Each reaction  
150 mixture (1 ml or 0.5 ml) contained 0.2 mM BV reduced with sodium dithionite, and variable concentrations  
151 of substrates in 50 mM MES, pH 6.0 buffer.

152 Reactions were started by the addition of RsMsrP enzyme (10 to 46 nM). Reduction of MetO rates were  
153 calculated from the  $\Delta A_{600\text{ nm}}$  slopes respecting a stoichiometry of 2 (2 moles of BV are oxidized for 1 mole  
154 of MetO reduced). Thus, the activity values presented as  $k_{\text{cat}}$  or  $k_{\text{obs}}$  ( $\text{s}^{-1}$ ) represent the number of moles of  
155 MetO reduced per mole of enzyme per second.

156 The apparent stoichiometry was determined similarly, using subsaturating concentrations of substrates:  
157 1–10  $\mu\text{M}$  oxidized  $\beta$ -casein, 1–10  $\mu\text{M}$  Met-*R*-O containing  $\beta$ -casein and 1.5–15  $\mu\text{M}$  Met-*S*-O containing  
158  $\beta$ -casein. The amount of oxidized BV was determined 1 hour after the addition of the RsMsrP (46 nM) by  
159 subtracting the final  $A_{600\text{ nm}}$  value from the initial one. Controls were done without the RsMsrP enzyme, or  
160 without the MetO-containing substrate. Quantities of MetO reduced were plotted as a function of substrate  
161 quantities and the apparent stoichiometry was obtained from the linear regression slope.

162 MsrA and MsrB activities were measured following the spectrophotometrical consumption of NADPH  
163 at 340 nm using the thioredoxin system similarly to the previously described protocol [15]. A 500- $\mu\text{l}$  reaction  
164 cuvette contained 200  $\mu\text{M}$  NADPH, 2  $\mu\text{M}$  TR1, 25  $\mu\text{M}$  Trx1 and 5  $\mu\text{M}$  MsrA or MsrB and 100  $\mu\text{M}$  oxidized  
165  $\beta$ -casein. Production of Met was calculated respecting a stoichiometry of 1 (1 mole of NADPH is oxidized  
166 for 1 mole of Met produced).

167 Analysis and kinetics parameters determination were done using GraphPad® Prism 4.0 software (La  
168 Jolla, CA, USA).

169

#### 170 **Electrospray ionization/Mass spectrometry analysis of purified proteins**

171 For oxidation, bovine  $\beta$ -casein (5  $\text{mg}\cdot\text{ml}^{-1}$ ) in 50 mM HEPES, pH 7.0, was incubated overnight at room  
172 temperature with  $\text{H}_2\text{O}_2$  (50 mM).  $\text{H}_2\text{O}_2$  was removed by desalting using a PD-10 column and the protein  
173 solution was concentrated with a 10-kDa cutoff Amicon® Ultra concentrator. Oxidized  $\beta$ -casein (100  $\mu\text{M}$ )  
174 was reduced by addition of 44 nM MsrP in a reaction mixture containing 50 mM HEPES pH 7.0, 0.8 mM  
175 BV and 0.2 mM sodium dithionite. After two hours of reaction in the glove-box, the repaired  $\beta$ -casein was  
176 analyzed by electrospray ionization/mass spectrometry in comparison to non-oxidized and oxidized  
177  $\beta$ -casein. Analyses were performed on a MicroTOF-Q Bruker (Wissembourg, France) with an electrospray

178 ionization source. Samples were desalted in ammonium acetate buffer (20 mM) and concentrated with a  
179 30-kDa cutoff Amicon® Ultra concentrator prior to analyses. Samples were diluted in CH<sub>3</sub>CN/H<sub>2</sub>O  
180 (1/1-v/v), 0.2% Formic Acid (Sigma). Samples were continuously infused at a flow rate of 3 μL.min<sup>-1</sup>. Mass  
181 spectra were recorded in the 50-7000 mass-to-charge (*m/z*) range. MS experiments were carried out with a  
182 capillary voltage set at 4.5 kV and an end plate off set voltage at 500 V. The gas nebulizer (N<sub>2</sub>) pressure  
183 was set at 0.4 bars and the dry gas flow (N<sub>2</sub>) at 4 L.min<sup>-1</sup> at a temperature of 190 °C. Data were acquired in  
184 the positive mode and calibration was performed using a calibrating solution of ESI Tune Mix (Agilent) in  
185 CH<sub>3</sub>CN/H<sub>2</sub>O (95/5-v/v). The system was controlled with the software package MicrOTOF Control 2.2 and  
186 data were processed with DataAnalysis 3.4.

187

#### 188 **Generation of *R. sphaeroides* 2.4.1 *msrP* mutant**

189 The *msrPQ* operon was amplified from *R. sphaeroides* 2.4.1 genomic DNA with the primers  
190 5'-AGATCGACACGCCATTCACC-3' and 5'-TCGGTGAGGCGCTATCTAGG-3'. The 2.2 kb PCR  
191 product was cloned into pGEMT Easy (Promega). An omega cartridge encoding resistance to streptomycin  
192 and spectinomycin [33] was then cloned into the *Bam*HI site of *msrP*. The resulting plasmid was digested  
193 with *Sac*I and the fragment containing the disrupted *msrP* gene was cloned into pJQ200mp18 [34]. The  
194 obtained plasmid, unable to replicate in *R. sphaeroides*, was transferred from *E. coli* by conjugation. The  
195 occurrence of a double-crossing over event was confirmed by PCR and absence of the protein from the  
196 SDS-PAGE profile.

#### 197 **Preparation of periplasmic samples for proteomics analysis**

198 *R. sphaeroides* 2.4.1 *msrP* mutant was grown under semi-aerobic conditions. Periplasmic extract was  
199 prepared as previously described [32] by cells incubation in 50 mM HEPES pH 8.0, 0.45 M sucrose, 1.3  
200 mM Ethylenediaminetetraacetic acid (EDTA) and 1 mg.ml<sup>-1</sup> chicken lysozyme. For Met oxidation, the  
201 periplasmic extract (0.7 mg.ml<sup>-1</sup>) was incubated with 20 mM *N*-Ethylmaleimide (NEM) and 2 mM NaOCl  
202 (Sigma-Aldrich) in 50 mM HEPES pH 8.0, 50 mM NaCl for 10 min at room temperature. NaOCl was

203 removed by desalting using a PD-10 column and buffer was changed to 50 mM MES pH 6.0. The protein  
204 solution was concentrated with a 3-kDa cutoff Amicon® Ultra concentrator. Three reaction mixtures were  
205 prepared in the glove box containing 35 µl of periplasmic extract, 1 mM benzyl viologen, 2 mM dithionite  
206 in 50 mM MES pH 6.0. The protein concentration in each reaction was 2.5 mg.ml<sup>-1</sup>. The first reaction  
207 contained non-oxidized periplasmic extract, the second and third ones contained oxidized periplasmic  
208 extract. For the third reaction (repaired periplasm) 10 µM RsMsrP was added. The reactions were incubated  
209 for three hours at room temperature.

### 210 **Trypsin proteolysis and tandem mass spectrometry**

211 Protein extracts were immediately subjected to denaturing PAGE electrophoresis for 5 min onto a 4–  
212 12% Bis-Tris gradient 10-well NuPAGE™ gel (Thermofisher). The proteins were stained with Coomassie  
213 Blue Safe solution (Invitrogen). Polyacrylamide bands corresponding to the whole proteomes were sliced  
214 and treated with iodoacetamide followed by trypsin as previously recommended [35]. Briefly, each band  
215 was destained with ultra-pure water, reduced with DTT, treated with iodoacetamide, and then proteolyzed  
216 with Gold Mass Spectrometry Grade Trypsin (Promega) in the presence of 0.01% ProteaseMAX surfactant  
217 (Promega). Peptides were immediately subjected to tandem mass spectrometry as previously recommended  
218 to avoid methionine oxidation [36]. The resulting peptide mixtures were analyzed in a data-dependent mode  
219 with a Q-Exactive HF tandem mass spectrometer (Thermo) coupled on line to an Ultimate 3000  
220 chromatography system chromatography (Thermo) essentially as previously described [37]. A volume of  
221 10 µL of each peptide sample was injected, first desalted with a reverse-phase Acclaim PepMap 100 C18  
222 (5 µm, 100 Å, 5 mm x 300 µm i.d., Thermo) precolumn and then separated at a flow rate of 0.2 µL.min<sup>-1</sup>  
223 with a nanoscale Acclaim PepMap 100 C18 (3 µm, 100 Å, 500 mm x 300 µm i.d., Thermo) column using  
224 a 150 min gradient from 2.5 % to 25 % of CH<sub>3</sub>CN, 0.1% formic acid, followed by a 30 min gradient from  
225 25% to 40% of CH<sub>3</sub>CN, 0.1% formic acid. Mass determination of peptides was done at a resolution of  
226 60,000. Peptides were then selected for fragmentation according to a Top20 method with a dynamic

227 exclusion of 10 sec. MS/MS mass spectra were acquired with an AGC target set at  $1.7 \cdot 10^5$  on peptides with  
228 2 or 3 positive charges, an isolation window set at 1.6  $m/z$ , and a resolution of 15,000.

### 229 **MS/MS spectrum assignment, peptide validation and protein identification**

230 Peak lists were automatically generated from raw datasets with Proteome Discoverer 1.4.1 (Thermo) and  
231 an in-house script with the following options: minimum mass (400), maximum mass (5,000), grouping  
232 tolerance (0), intermediate scans (0) and threshold (1,000). The resulting .mgf files were queried with the  
233 Mascot software version 2.5.1 (Matrix Science) against the *R. sphaeroides* 241 annotated genome database  
234 with the following parameters: full-trypsin specificity, up to 2 missed cleavages allowed, static modification  
235 of carbamidomethylated cysteine, variable oxidation of methionine, variable deamidation of asparagine and  
236 glutamine, mass tolerance of 5 ppm on parent ions and mass tolerance on MS/MS of 0.02 Da. The decoy  
237 search option of Mascot was activated for estimating the false discovery rate (FDR) that was below 1%.  
238 Peptide matches with a MASCOT peptide score below a P value of 0.05 were considered. Proteins were  
239 validated when at least two different peptides were detected. The FDR for proteins was below 1% as  
240 estimated with the MASCOT reverse database decoy search option.

### 241 **Ice logo analysis**

242 Ice logo analysis were performed using the IceLogo server  
243 (<http://iomics.ugent.be/icelogoserver/index.html>) [38].

244

245

## 246 **Results**

### 247 **The *R. sphaeroides* MsrP is an efficient protein-MetO reductase**

248 The results showing that the EcMsrP is a protein-bound MetO reductase, able to reduce both *R*- and  
249 *S*-diastereomer of MetO [28] prompted us to evaluate whether these properties are conserved for RsMsrP.  
250 As the EcMsrP was determined to be 5-fold less efficient in reducing the Met-*S*-O than Met-*R*-O, and  
251 knowing that all previously identified MetO reductases were absolutely stereospecific towards one  
252 enantiomer, we thought that it cannot be excluded that a protein contamination might explain the apparent  
253 ability of the EcMsrP to reduce the Met-*S*-O [28]. Such potential Met-*S*-O reductase contaminant should be  
254 able to use benzyl viologen (BV) as electron provider in activity assays and a good candidate is the  
255 periplasmic DMSO reductase [26,27]. Thus, we prepared the recombinant RsMsrP from a *R. sphaeroides*  
256 strain devoid of the *dorA* gene encoding the catalytic subunit of the DMSO reductase [32]. After purification  
257 on Ni-affinity column and removal of the polyhistidine tag, the mature enzyme was purified by gel filtration,  
258 followed by strong anion exchange, yielding a highly pure enzyme (Supplementary Figure S1).

259 After optimal pH determination showing that RsMsrP acts efficiently between pH 5.5 and 8.0  
260 (Supplementary Figure S2), we determined the kinetic parameters of RsMsrP using BV as an electron  
261 provider and several model substrates: the free amino acid MetO, a synthetic tripeptide Ser-MetO-Ser and  
262 the oxidized bovine  $\beta$ -casein (Table 1). The  $\beta$ -casein contains 6 Met, it is intrinsically disordered, and was  
263 shown as an efficient substrate for the yeast MsrA and MsrB, after oxidation [15] (see also Supplementary  
264 Figure S3). Commercial  $\beta$ -casein contains a mixture of genetic variants, appearing as multiple peaks on  
265 mass spectrometry (MS) spectra (Figure 1A). After oxidation with H<sub>2</sub>O<sub>2</sub>, MS analysis confirmed an increase  
266 in mass of 96 Da for each peak, very likely corresponding to the addition of 6 oxygen atoms on the Met  
267 residues (Figure 1B). Using the free MetO, we determined a  $k_{\text{cat}}$  of  $\sim 122 \text{ s}^{-1}$  and a  $K_{\text{m}}$  of  $\sim 115,000 \mu\text{M}$ ,  
268 yielding a catalytic efficiency ( $k_{\text{cat}}/K_{\text{m}}$ ) of  $\sim 1,000 \text{ M}^{-1} \cdot \text{s}^{-1}$  (Table 1). With the Ser-MetO-Ser peptide, the  $k_{\text{cat}}$   
269 and the  $K_{\text{m}}$  values were  $\sim 108 \text{ s}^{-1}$  and  $\sim 13,000 \mu\text{M}$ , and thus the  $k_{\text{cat}}/K_{\text{m}}$  was  $\sim 8,300 \text{ M}^{-1} \cdot \text{s}^{-1}$ . Compared to  
270 free MetO, the  $\sim 8$ -fold increase in catalytic efficiency is due to the lower  $K_{\text{M}}$ , and thus this indicates that

271 the involvement of the MetO in peptide bonds increases its ability to be reduced by RsMsP. With the  
272 oxidized  $\beta$ -casein, the  $k_{cat}$  and the  $K_m$  were  $\sim 100 \text{ s}^{-1}$  and  $\sim 90 \text{ }\mu\text{M}$ , respectively. The  $k_{cat}/K_m$  was thus  $\sim$   
273  $1,000,000 \text{ M}^{-1}\cdot\text{s}^{-1}$ . This value, 4 orders of magnitude higher than the one determined with free MetO,  
274 indicates that the oxidized protein is a far better substrate for RsMsP. Moreover, even assuming that all  
275 MetO in the oxidized  $\beta$ -casein were equal substrates for the RsMsP and thus multiplying the  $K_M$  by 6, the  
276 catalytic efficiency obtained ( $\sim 175,000 \text{ M}^{-1}\cdot\text{s}^{-1}$ ) remained  $\sim 175$ -fold higher for the oxidized protein than  
277 for the free amino acid. These results indicate that the RsMsP acts effectively as a protein-MetO reductase.

### 278 **RsMsP reduces both Met-*R*-O and Met-*S*-O of an oxidized model protein**

279 To determine whether the RsMsP can reduce both MetO diastereomers, we chose the oxidized bovine  
280  $\beta$ -casein as a model substrate because it was efficiently reduced by the yeast MsrA and MsrB indicating the  
281 presence of both *R* and *S* diastereomers of MetO [15]. After oxidation with  $\text{H}_2\text{O}_2$ , we treated the protein  
282 with MsrA and MsrB, taking advantage of their stereospecificity, to obtain protein samples containing only  
283 the Met-*R*-O (" *$\beta$ -casein-R-O*") or the Met-*S*-O (" *$\beta$ -casein-S-O*"), respectively. The absence of one or the  
284 other diastereomer of MetO was validated by the absence of remaining Msr activity (Supplementary Figure  
285 3). These three forms, containing either two or only one diastereomer of MetO, were tested as substrate for  
286 RsMsP (Figure 2). We measured a  $k_{cat}$  of  $\sim 45 \text{ s}^{-1}$  with the oxidized  $\beta$ -casein, which decreased to  $\sim 30$  and  
287 to  $5 \text{ s}^{-1}$  for the  $\beta$ -casein containing the *R* or the *S* sulfoxide, respectively. This result shows that RsMsP can  
288 reduce both diastereomers of MetO, but appears 6-fold less efficient to reduce Met-*S*-O than Met-*R*-O.

289 From this result, we postulated that RsMsP should be able to reduce all MetO in the oxidized  $\beta$ -casein,  
290 as this protein was intrinsically disordered and thus all MetO were very likely accessible. We evaluated this  
291 hypothesis by mass spectrometry analysis. When incubated with RsMsP, the mass of the oxidized protein  
292 decreased by 96 Da, showing that all MetO were reduced (Figure 1C). Altogether, these results clearly  
293 showed that RsMsP was able to reduce both *R*- and *S*-diastereomers of MetO contained in the oxidized  
294  $\beta$ -casein, and thus lacked stereospecificity.

295

296 **The RsMsrP preferentially reduces Met-R-O but acts effectively on Met-S-O too**

297 To gain insight into the substrate preference of RsMsrP toward one of the diastereomers of MetO, we  
298 performed kinetics analysis using the oxidized  $\beta$ -casein containing the *R* or *S* diastereomers of MetO (Table  
299 1; Supplementary Figure S4). With the protein containing only the *R*-diastereomer of MetO  
300 (“ $\beta$ -casein-*R*-O”), we determined a  $k_{\text{cat}}$  of  $\sim 50 \text{ s}^{-1}$ , a  $K_m$  of  $\sim 50 \mu\text{M}$  and thus a catalytic efficiency of  $\sim$   
301  $950,000 \text{ M}^{-1} \cdot \text{s}^{-1}$ . In the case of the protein containing only the Met-*S*-O (“ $\beta$ -casein-*S*-O”), the  $k_{\text{cat}}$  and  $K_m$   
302 were  $\sim 8 \text{ s}^{-1}$  and of  $\sim 50 \mu\text{M}$ , respectively. This yielded a catalytic efficiency of  $142,000 \text{ M}^{-1} \cdot \text{s}^{-1}$ . This value,  
303  $\sim 7$  fold lower than the one obtained with the  $\beta$ -casein-*R*-O, was due to the lower  $k_{\text{cat}}$  as the  $K_m$  was not  
304 changed. These values seem to indicate that the RsMsrP preferentially reduced the *R* than the *S* diastereomer  
305 of MetO in the oxidized  $\beta$ -casein. However, as we could not exclude that the proportion of Met-*R*-O was  
306 higher than the proportion of Met-*S*-O in the protein, we developed an assay to estimate the number of MetO  
307 reduced by RsMsrP in the three forms of oxidized  $\beta$ -casein. We measured the total moles of BV consumed  
308 for the reduction of all MetO using subsaturating concentrations of the oxidized protein. Practically, the  
309 absorbance at 600 nm was measured before and 90 min after substrate addition. As two moles of BV are  
310 consumed per mole of MetO reduced, we obtained the apparent stoichiometry of RsMsrP toward the  
311 oxidized protein by performing a linear regression on the straight part of the line and taking the slope, which  
312 defines the amount of MetO reduced as a function of substrate concentration (Figure S5). The values  
313 determined were  $\sim 4.6$ ,  $\sim 3.2$  and  $\sim 1.8$  for the oxidized  $\beta$ -casein, the  $\beta$ -casein-*R*-O and the  $\beta$ -casein-*S*-O,  
314 respectively. In the case of the oxidized  $\beta$ -casein, we expected a value of 6 based on the data obtained by  
315 mass spectrometry (Figure 1). This may have been due to the heterogeneity of the oxidized  $\beta$ -casein (all  
316 Met were not initially fully oxidized) and/or to a too short time of incubation (all MetO were not fully  
317 reduced, as indicated by the presence of a peak corresponding to a portion of  $\beta$ -casein not fully reduced in  
318 Figure 1C). To compare the catalytic parameters, the data was normalized by multiplying the  $K_m$  by the  
319 apparent stoichiometries, yielding values per reduced MetO, thereby allowing the removal of variation due  
320 to the different numbers of reduced Met-*R*-O or Met-*S*-O. The catalytic efficiencies were thus 230,000,  
321 300,000 and  $80,000 \text{ M}^{-1} \cdot \text{s}^{-1}$  for the oxidized  $\beta$ -casein, the  $\beta$ -casein-*R*-O and the  $\beta$ -casein-*S*-O, respectively

322 (Table 1). The highest value was that obtained for the  $\beta$ -casein containing only the *R* form of MetO,  
323 indicating that this diastereomer was the preferred substrate for RsMsP. However, the value obtained with  
324 the  $\beta$ -casein-*S*-O was only less than 4-fold lower, showing that RsMsP can also act effectively on the  
325 Met-*S*-O.

### 326 **RsMsP can reduce a broad spectrum of periplasmic proteins**

327 To identify potential periplasmic substrates of RsMsP and gain insight into its substrate specificity, we  
328 applied a high-throughput shotgun proteomic strategy. Periplasmic proteins from the *mrsP* *R. sphaeroides*  
329 mutant were extracted, oxidized with NaOCl and then reduced *in vitro* with recombinant RsMsP. Untreated  
330 periplasmic proteins, oxidized periplasmic proteins and RsMsP-treated oxidized periplasmic proteins were  
331 analyzed by semi-quantitative nanoLC–MS/MS. All experiments were done systematically for 3 biological  
332 replicates and resulted in the identification of 362,700 peptide-to-spectrum matches. From all 11,320  
333 individual peptide sequences, we identified 2,553 unique Met belonging to 720 proteins. The overall  
334 percentages of Met oxidation were ~ 35%, ~ 71% and ~ 40% for proteins from the periplasm extract, the  
335 oxidized periplasm extract and the RsMsP-repaired proteins, respectively (Supplementary Table 1). This  
336 first result indicates that RsMsP is very likely able to reduce MetO from numerous proteins and to restore  
337 an oxidation rate similar to the one of the periplasmic extract that has not undergone any oxidation.

338 The identification of preferential RsMsP substrates requires the precise comparison of the oxidation  
339 state of Met residues from periplasmic proteins before and after the action of the enzyme. After tryptic  
340 digestion, since most of the Met/MetO-containing peptides were found in low abundance (*i.e.* with very low  
341 spectral counts), we focused on the proteins robustly detected in all samples. We selected the Met-containing  
342 peptides for which at least 10 spectral counts were detected in two replicates for each condition (*i.e.*  
343 untreated periplasm, oxidized periplasm and repaired oxidized periplasm) and at least 7 spectral counts were  
344 found in the third replicate. This restricted the dataset to 202 unique Met belonging to 70 proteins  
345 (Supplementary Table 2). Overall percentage of Met oxidation (calculated as the number of spectral counts  
346 for a MetO-containing peptide vs. the total number of spectral count for this peptide) varied from 2% to

347 87%, from 9% to 100% and from 4% to 91% in the periplasm, oxidized periplasm and repaired oxidized  
348 periplasm, respectively. Comparison of Met-O containing peptides between oxidized and RsMsrP treated  
349 samples indicates that the percentage of reduction varied from 100 % to no reduction at all. Eleven MetO  
350 were not reduced and 22 were reduced at more than 75 % (only 2 at 100 %). The percentage of reduction  
351 for the remaining majority of MetO was almost uniformly distributed between inefficient (less than 25 %)  
352 to efficient (75% or more) reduction (Figure 3A).

353 No clear evidence of sequence or structure characteristic arose from these 70 identified proteins, neither  
354 in term of size or in Met content (Supplementary Table 2). The periplasmic chaperone SurA, the  
355 peptidyl-prolyl cis-trans isomerase PpiA, the thiol-disulfide interchange protein DsbA, the  
356 spermidine/putrescine-binding periplasmic protein PotD and the ProX protein were previously proposed as  
357 potential substrates of EcMsrP [28]. All these proteins contain at least one MetO amongst the most  
358 efficiently reduced by RsMsrP (Supplementary Table 2), indicating that they are potential conserved  
359 substrates of the MsrP enzymes in *E. coli* and *R. sphaeroides*, and very likely in numerous other  
360 gram-negative bacteria.

361 The sensitivity to oxidation of the Met belonging to these 70 proteins, and their efficiency of reduction  
362 by RsMsrP show a wide range of variation, from Met highly sensitive to oxidation and efficiently reduced  
363 to Met barely sensitive to NaOCl treatment and not reduced by RsMsrP (Supplementary Table 2). Moreover,  
364 this diversity could be visible within a single protein, in which all Met may not be uniformly oxidized and  
365 reduced. For instance, the ABC transporter DdpA, along with another putative ABC transporter (Figure  
366 3B,C), contained one of the two only MetO found to be fully reduced in the dataset (Met-230 and Met-353,  
367 respectively), although DdpA also contained the Met-243 that was neither efficiently oxidized nor reduced.  
368 This is also illustrated by the case of the peptidyl-prolyl cis-trans isomerase, which possessed the Met found  
369 to have the higher decrease in oxidation in the entire dataset (Met-172) but also a Met almost not reduced  
370 by RsMsrP (Met-190) (Figure 3D). The Met-539 of the PQQ dehydrogenase XoxF illustrates the case in  
371 which a Met was highly sensitive to NaOCl-oxidation and very efficiently reduced (Figure 3E). Twenty-one  
372 Met were oxidized at 50 % or more and reduced by 50 % or more by RsMsrP (Supplementary Table S2).

373 Altogether, these results show that RsMsrP can reduce a broad spectrum of apparently unrelated proteins  
374 (only 11 Met among 202 were not reduced). However, since all MetO were not reduced with similar  
375 efficiency, some structural or sequence determinants could drive the ability of MetO to be reduced by  
376 RsMsrP.

### 377 **The nature of the amino acids surrounding a MetO influences the RsMsrP efficiency**

378 Having in hand a relatively large dataset of oxidized and reduced Met prompted us to search for  
379 consensus sequences that could favor or impair the oxidation of a Met or the reduction of a MetO by RsMsrP.  
380 For all identified Met, we extracted, the surrounding 5 amino acids on the N- and C-terminal sides to obtain  
381 an 11-amino acid sequence with the considered Met centered at the 6<sup>th</sup> position. As shown for bacterial  
382 MsrB [39], this length might be sufficient to encompass the amino acids in physical contact with RsMsrP  
383 during reduction. We then performed an IceLogo analysis aiming to identify whether some residues were  
384 enriched or depleted around the target Met. The principle is to compare a ‘positive’ dataset of peptides, to a  
385 ‘negative’ one [38]. To find potential consensus sequences of oxidation, we first compared all unique  
386 MetO-containing peptides from both the untreated and the NaOCl-oxidized periplasmic extracts (our  
387 positive dataset) to the theoretical *R. sphaeroides* proteome (our negative dataset). The IceLogo presented  
388 in Figure 4A shows that MetO-containing sequences were mainly depleted of His and aromatic or  
389 hydrophobic residues (Trp, Phe, Tyr, Leu, Ile) and were mainly enriched in polar or charged amino acids  
390 (Asn, Gln, Asp, Glu and Lys). This suggests that Met in a polar environment, as commonly found at the  
391 surface of proteins, are very likely more susceptible to oxidation than those located in hydrophobic  
392 environments such as those in the protein core. We then compared all these unique MetO-containing  
393 peptides to all the Met-containing peptides from the same samples (Figure 4B), and we observed that Trp,  
394 along with His, Tyr and Cys, were principally depleted around the potentially oxidized Met. Strikingly, the  
395 only amino acid significantly more abundant around an oxidized Met was another Met in position -2 and  
396 +2. These results indicate that oxidation sensitive Met might be found as clusters.

397 To identify potential consensus sequence favorable to MetO reduction by RsMsP, we performed a  
398 precise comparison of the oxidation percentage before and after the action of the enzyme. We thus defined  
399 two criteria to characterize the reduction state of each Met: i) the percentage of reduction calculated using  
400 the formula described in Supplementary Table S2 and based on the comparison of the oxidation percentages  
401 in oxidized versus repaired oxidized periplasm. For instance, a Met found oxidized at 25 % in the oxidized  
402 periplasm and at 5 % in the repaired oxidized periplasm was considered enzymatically reduced at 80 %. ii)  
403 the decrease in percentage of oxidation by comparison of the 2 samples. For instance, the same Met found  
404 oxidized at 25 % in the oxidized periplasm and 5 % in the repaired extract had a decrease in the oxidation  
405 percentage of 20 %. This second criterion was used to avoid bias in which very little oxidized Met were  
406 considered as efficient substrates (*i.e.* a Met oxidized at 5 % in the oxidized periplasm extract and at 1 % in  
407 the repaired oxidized periplasm was reduced at 80 %, similarly to one passing from 100 % to 20 %, which  
408 intuitively appears as a better substrate than the previous one). We selected as efficiently and inefficiently  
409 reduced MetO those for which both criteria were higher than 50 % and lower than 10 %, respectively.  
410 Comparison of the sequences surrounding the efficiently reduced MetO to the theoretical proteome of *R.*  
411 *sphaeroides* showed no depletion of amino acid, but mainly enrichment of polar amino acids (Gln, Lys, and  
412 Glu) around the oxidized Met (Figure 5A). Similar analysis with the inefficiently reduced MetO indicated  
413 the enrichment of Thr and Ser in the far N-terminal positions (-5 and -4) and of a Tyr in position -2 (Figure  
414 5B). The C-terminal positions (+ 1 to +5) were mainly enriched in charged amino acids (Gln, Lys, and Glu),  
415 similarly to efficiently reduced MetO. This apparent contradiction may indicate that the amino acids in the  
416 C-terminal position of the considered MetO did not really influence the efficiency of RsMsP but were  
417 observed simply because of the inherent composition of the overall identified peptides. We then compared  
418 the variation of amino acids composition of the MetO-containing peptides between both datasets, using the  
419 inefficiently reduced MetO as a negative dataset (Figure 5C). The results were similar to those obtained by  
420 comparison with the entire theoretical proteome of the bacterium, *i.e.* most enriched amino acids were polar  
421 (Glu, Gln, Asp and Lys) at most extreme positions (-5, -4 and + 2 to + 5). Of note, the conserved presence  
422 of a Gly in position -1, and the presence of several other Met around the central Met. This potential

423 enrichment of Met around an oxidation site is consistent with the result found for the sensibility of oxidation  
424 (Figure 4B), and indicates that potential clusters of MetO could be preferred substrates for RsMsrP. We  
425 found 16 peptides containing 2 or 3 MetO, reduced at more than 25 % by RsMsrP (Supplementary Table  
426 S2). This was illustrated, for example, by the cell division coordinator CpoB which possesses two close Met  
427 residues (66 and 69) highly reduced by the RsMsrP, or by the uncharacterized protein (YP\_353998.1) having  
428 4 clusters of MetO reduced by the RsMsrP (Supplementary Table S2).

429 From this analysis, the only depleted amino acids appeared to be Thr and Pro in positions -4 and -3  
430 (Figure 4C). To validate these results, we designed two peptides, QWGAGM(O)QAEED and  
431 TTPGYM(O)EEWNK, as representative of most efficiently and most inefficiently RsMsrP-reduced  
432 peptide-containing MetO, respectively. We used them as substrates to determine reduction kinetics  
433 parameters for RsMsrP (Table 1; Supplementary Figure S6). The results showed that the peptide  
434 QWGAGM(O)QAEED was efficiently reduced, with the highest  $k_{cat}$  value from all the substrates we tested  
435 ( $\sim 480 \text{ s}^{-1}$ ) and a  $K_m$  of  $\sim 4,500 \mu\text{M}$ . This yielded a  $k_{cat}/K_m$  of  $\sim 100,000 \text{ M}^{-1} \cdot \text{s}^{-1}$ , which is 2 orders of magnitude  
436 higher than the one determined for the free MetO, and 10-fold lower than for the oxidized  $\beta$ -casein (Table  
437 1). On the contrary, the peptide TTPGYM(O)EEWNK was not efficiently reduced by RsMsrP (Table 1;  
438 Supplementary Figure S6). Indeed, we could not determine the kinetic parameters as the activity value curve  
439 never reached an inflection point using concentrations as high as  $5,000 \mu\text{M}$ . The maximal  $k_{cat}$  value was  
440 determined at  $\sim 70 \text{ s}^{-1}$  at  $5,000 \mu\text{M}$  of peptide, which is  $\sim 3.5$ -fold less than the one determined with the  
441 same concentration of the other peptide ( $\sim 250 \text{ s}^{-1}$ ) (Supplementary Figure S6). These results are in full  
442 agreement with the proteomics analysis and confirm that the nature of the amino acids surrounding a MetO  
443 in a peptide or a protein strongly influences its ability to be reduced by RsMsrP.

#### 444 **The RsMsrP preferentially reduces unfolded oxidized proteins**

445 To test whether structural determinants affect RsMsrP efficiency of MetO reduction, we compared its  
446 activity using oxidized model proteins, either properly folded or unfolded. We started with chicken  
447 lysozyme as it is a very well folded protein highly stabilized by four disulfide bonds [40]. We oxidized it

448 with H<sub>2</sub>O<sub>2</sub> and checked its oxidation state by mass spectrometry (Supplementary Figure S7). Surprisingly,  
449 using a protocol similar to the one allowing the complete oxidation of the 6 Met of  $\beta$ -casein, we observed  
450 only a weak and incomplete oxidation of the protein. The major peak corresponded to the non-oxidized form  
451 and a small fraction had an increase in mass of 16 Da, likely corresponding to the oxidation of one Met.  
452 Nevertheless, we prepared from this oxidized sample, an unfolded oxidized lysozyme by reduction with  
453 dithiothreitol in 4M urea followed by iodoacetamide alkylation of cysteines, and both samples (oxidized  
454 and unfolded oxidized), were used as substrates for RsMsrP (Figure 6). We also used  
455 glutathione-*S*-transferase (GST) which possesses 9 Met and is highly structured. After oxidation with H<sub>2</sub>O<sub>2</sub>,  
456 GST was incubated with 4 M of the chaotropic agent urea, a concentration sufficient to induce complete  
457 unfolding of the protein [15]. For both oxidized proteins, we observed a dramatic increase in activity after  
458 unfolding. Indeed, the RsMsrP activity increased 7-fold with the unfolded oxidized lysozyme compared to  
459 the folded one, and 6-fold in the case of the unfolded oxidized GST compared to the folded oxidized GST  
460 (Figure 6). As the unfolded oxidized protein solutions of lysozyme or GST contained a substantial amount  
461 of urea, we performed controls in which the urea was added extemporaneously in the cuvette during the  
462 measurements, showing that urea did not influence the RsMsrP activity (Supplementary Figure S8).

463 Mass spectrometry analysis showed that the RsMsrP was able to completely reduce the oxidized  
464 lysozyme in these conditions (Supplementary Figure S7), suggesting that observed differences of repair  
465 between the folded- and unfolded-oxidized lysozyme were not due to the incapacity of RsMsrP to reduce  
466 some MetO, but were due to kinetic parameters. We thus determined the kinetics of reduction of these  
467 proteins by RsMsrP (Table 1, Supplementary Figure S8). For the oxidized lysozyme, the  $k_{\text{cat}}$  and the  $K_{\text{m}}$   
468 were  $\sim 4 \text{ s}^{-1}$  and  $\sim 900 \mu\text{M}$ , respectively. Using the unfolded oxidized lysozyme, the  $k_{\text{cat}}$  increased to  $\sim 7 \text{ s}^{-1}$   
469 and the  $K_{\text{m}}$  decreased to  $\sim 100 \mu\text{M}$ . The catalytic efficiency determined with the unfolded oxidized lysozyme  
470 was thus  $\sim 18$ -fold higher than the one determined using the oxidized lysozyme before unfolding ( $70,200$   
471 vs.  $4,000 \text{ M}^{-1} \cdot \text{s}^{-1}$ ). Similar results were obtained with GST. Indeed, with the oxidized GST, we recorded  $k_{\text{cat}}$   
472 and  $K_{\text{m}}$  values of  $\sim 8 \text{ s}^{-1}$  and  $\sim 640 \mu\text{M}$ , respectively. Whereas for the unfolded oxidized GST, the  $k_{\text{cat}}$  was  
473 slightly higher ( $\sim 12 \text{ s}^{-1}$ ), and the  $K_{\text{m}}$  was  $\sim 6$ -fold lower ( $\sim 100 \mu\text{M}$ ). The catalytic efficiency was 10-fold

474 higher for the unfolded oxidized GST than for its folded counterpart (Table 1; Supplementary Figure S8).  
475 Altogether, these results showed that RsMsrP is more efficient at reducing MetO in unfolded than in folded  
476 oxidized proteins. Moreover, as evidenced with lysozyme that contained only one MetO in our conditions,  
477 the increase in activity using unfolded substrate is not dependent on the number of MetO reduced.

## 478 Discussion

479 All organisms have to face harmful protein oxidation and almost all possess canonical Msrs that protect  
480 proteins by reducing MetO. Bacteria also have molybdoenzymes able to reduce MetO, as a free amino acid  
481 for the DMSO reductase [26] or the biotin sulfoxide reductase BisC/Z [24,25], but also included in proteins  
482 in the case of MsrP [28,29]. Genetic studies and the conservation of MsrP in most gram-negative bacteria  
483 indicate that it is very likely a key player in the protection of periplasmic proteins against oxidative stress  
484 [28,29] However, an in-depth characterization of its protein substrate specificity is still lacking. In this work,  
485 we chose the MsrP from the photosynthetic purple bacteria *R. sphaeroides* as a model enzyme to uncover  
486 such specificity. Using purified oxidized proteins and peptides, we showed that RsMsrP is a very efficient  
487 protein-containing MetO reductase, with apparent affinities ( $K_m$ ) for oxidized proteins 10 to 100-fold lower  
488 than for the tripeptide Ser-MetO-Ser or the free MetO (Table 1). As reported for canonical MsrA and MsrB  
489 [15], we observed important variations in the reduction  $k_{cat}$  of different oxidized proteins, arguing for the  
490 existence of sequence and structural determinants affecting the enzyme efficiency (Table 1).

491 To find potential physiological substrates of RsMsrP and uncover their properties, we used a proteomic  
492 approach aiming at comparing the oxidation state of periplasmic proteins after treatment with the strong  
493 oxidant NaOCl, followed by RsMsrP reduction of these proteins. We found 202 unique Met, belonging to  
494 70 proteins, for which the sensitivity of oxidation and the ability to serve as an RsMsrP substrate varied  
495 greatly (Figure 3, Supplementary Table S2). MetO efficiently reduced by RsMsrP belong to structurally and  
496 functionally unrelated proteins, indicating that RsMsrP very likely does not possess specific substrates and  
497 acts as a global protector of protein integrity in the periplasm. Interestingly, we observed from our IceLogo  
498 analysis that Met sensitive to oxidation are generally presented in a polar amino acid environment and can  
499 be found in clusters (Figure 4). These properties might be common to all Met in proteins as similar results  
500 were found in human cells [41,42] and plants [43]. Moreover, oxidized Met efficiently reduced by the  
501 RsMsrP were also found clustered in polar environments and our analysis shows that the presence of Thr  
502 and Pro in N-terminal side of a MetO strongly decrease RsMsrP efficiency (Table 1, Figure 5 and

503 Supplementary Figure S6). To our knowledge, the presence of a Thr close to a MetO was not previously  
504 shown to influence any Msr activity, but the presence of a Pro was shown to decrease or totally inhibit MetO  
505 reduction by the human MsrA and MsrB3, depending on its position [41].

506 The presence of oxidation-sensitive Met efficiently reduced by the RsMsrP in clusters on polar parts of  
507 proteins should facilitate the oxidation/reduction cycle aiming to scavenge ROS as previously proposed for  
508 canonical Msrs [44]. This is also illustrated by the methionine-rich protein MrpX proposed as main substrate  
509 of the *A. suillum* MsrP, which is almost only composed of Met, Lys, Glu and Asp [29]. The presence of  
510 numerous MetO on a single molecule of protein substrate should increase the RsMsrP efficiency as one  
511 molecule of the substrate allows several catalytic cycles, potentially without breaking physical contact  
512 between the enzyme and its substrate.

513 Comparison of the RsMsrP activity using folded or unfolded protein substrates (lysozyme and GST)  
514 showed that it is far more efficient to reduce unfolded oxidized proteins (Figure 6). Similar results were  
515 found for canonical Msrs [15]. In the case of MsrB it was because more MetO were accessible for reduction  
516 whereas for MsrA this increase was independent of the number of MetO reduced. Here, the use of lysozyme  
517 containing only one MetO (Supplementary Figure S7) undoubtedly showed that the increase in activity is  
518 not related to the unmasking of additional MetO upon protein denaturation (Table 1; Figure 6). This could  
519 indicate that the RsMsrP has better access to the MetO in the protein or that the MetO is more easily  
520 accommodated in the active site of the enzyme because of increased flexibility. This should provide a  
521 physiological advantage to the bacteria during oxidative attacks, which could occur during other stresses  
522 such as acid or heat, hence promoting simultaneous oxidation and unfolding of proteins. Particularly,  
523 hypochlorous acid, which was shown to induce *msrP* expression in *E. coli* [28] and *A. suillum* [29], has  
524 strong oxidative and unfolding effect on target proteins [45].

525 Finally, previous work indicated that the *E. coli* MsrP lacks stereospecificity and can reduce both *R*- and  
526 *S*-diastereomers of MetO chemically isolated from a racemic mixture of free L-Met-*R,S*-O [28]. This  
527 discovery is of fundamental importance as it breaks a paradigm in Met oxidation and reduction knowledge,

528 and very likely for all enzymology as non-stereospecific enzymes were very rarely described. Indeed, to our  
529 knowledge, all previously characterized enzymes able to reduce Met sulfoxide or related substrates were  
530 shown to be absolutely stereospecific. This was the case for the canonical MsrA and MsrB, which reduce  
531 only the *S*-diastereomer and the *R*-diastereomer, respectively [7,9–14], as well as for the free Met-*R*-O  
532 reductase [22,23] and for the DMSO reductase [26,27] and BisC/Z molybdoenzymes [24,25]. To evaluate  
533 the potential lack of stereospecificity of the RsMsrP, we chose to use a different strategy than the one used  
534 for *E. coli* MsrP [28] and prepared oxidized  $\beta$ -casein containing only one or the other MetO diastereomer  
535 using yeast MsrA and MsrB to eliminate the *S*- and the *R*-diastereomers, respectively. Activity assays and  
536 kinetic experiments using a highly purified RsMsrP demonstrated that it can efficiently reduce the  $\beta$ -casein  
537 containing only the *R*- or the *S*-diastereomer (Table 1; Figure 2 and Supplementary Figure S4). Moreover,  
538 this lack of stereospecificity was undoubtedly confirmed by the ability of the RsMsrP to reduce all 6 MetO  
539 formed on the oxidized  $\beta$ -casein (Figure 1). These results, consistent with Gennaris and coworkers finding,  
540 indicate that this lack of stereospecificity is very likely common to all MsrP homologs. Together with the  
541 apparent ability of the enzyme to repair numerous unrelated oxidized proteins, the capacity to reduce both  
542 diastereomers of MetO, argues for a role of MsrP in the general protection of envelope integrity in gram  
543 negative bacteria. However, it raises questions regarding the structure of its active site as the enzyme should  
544 be able to accommodate both diastereomers. From this, we wondered whether the RsMsrP could reduce the  
545 Met sulfone, which can be imagined as a form of oxidized Met containing both *R*- and *S*-diastereomers, but  
546 we did not detect any activity (Supplementary Figure S9). Although it could be because of an incompatibility  
547 in redox potential, it may indicate that this form of oxidized Met cannot reach the catalytic atom. The  
548 three-dimensional structure of the oxidized form of *E. coli* MsrP indicated that the molybdenum atom, which  
549 is supposed to be the catalytic center of the enzyme, is buried 16 Å from the surface of the protein [46]. The  
550 next challenge will be to understand the MsrP reaction mechanism and will require the determination of the  
551 enzyme structure in its oxidized and reduced forms bound to its MetO-containing substrates.

552

553 **Acknowledgment:** We are very grateful to Prof. Vadim, N. Gladyshev (Brigham's and Women Hospital  
554 and Harvard Medical School) for the gift of pET28a-MsrA, pET21b-MsrB, pET15b-TR1, pET15b-Trx1  
555 and pGEX4T1 expression vectors. We thank Dr. Benjamin Ezraty and the members of his team (Laboratoire  
556 de Chimie Bactérienne, Institut de Microbiologie de la Méditerranée) for fruitful discussions. Pascaline  
557 Auroy-Tarrago (Laboratoire de Bioénergétique et Biotechnologie des Bactéries et Microalgues, CEA,  
558 BIAM) is acknowledged for her help with proteomics analysis.

559  
560 **Competing Interests:** The Authors declare that there are no competing interests associated with the  
561 manuscript.

562  
563 **Funding:** This work was supported by the Commissariat à l'Energie Atomique et aux Energies Alternatives  
564 (CEA) and by the project METOXIC (ANR 16-CE11-0012).

565  
566 **Author contribution:** LT, PA, DP and MS designed the study. LT, SG, MIS and MS purified RsMsrP. LT  
567 and MS prepared all other proteins. LT, SG, MIS, MS performed biochemical characterization of RsMsrP.  
568 LT, MS and DL performed  $\beta$ -casein and lysozyme mass spectrometry analysis and analyzed the data. SG  
569 and MS prepared *R. sphaeroides* 2.4.1 *msrP* mutant and periplasmic proteins samples. BA, GM and JA  
570 performed proteomics analysis of periplasmic proteins and LT, MS, GM and JA analyzed the data. LT wrote  
571 the manuscript with contribution of MIS, DL, PA, DP, JA and MS. All authors approved the final  
572 manuscript.

- 574 1 Messner, K. R. and Imlay, J. A. (1999) The identification of primary sites of superoxide and  
575 hydrogen peroxide formation in the aerobic respiratory chain and sulfite reductase complex  
576 of *Escherichia coli*. *J. Biol. Chem.* **274**, 10119–10128.
- 577 2 Glaeser, J., Nuss, A. M., Berghoff, B. A. and Klug, G. (2011) Singlet oxygen stress in  
578 microorganisms. *Adv. Microb. Physiol.* **58**, 141–173.
- 579 3 Ezraty, B., Gennaris, A., Barras, F. and Collet, J.-F. (2017) Oxidative stress, protein damage  
580 and repair in bacteria. *Nat. Rev. Microbiol.* **15**, 385–396.
- 581 4 Imlay, J. A. (2013) The molecular mechanisms and physiological consequences of oxidative  
582 stress: lessons from a model bacterium. *Nat. Rev. Microbiol.* **11**, 443–454.
- 583 5 Ziegelhoffer, E. C. and Donohue, T. J. (2009) Bacterial responses to photo-oxidative stress.  
584 *Nat. Rev. Microbiol.* **7**, 856–863.
- 585 6 Davies, M. J. (2005) The oxidative environment and protein damage. *Biochim. Biophys.*  
586 *Acta* **1703**, 93–109.
- 587 7 Sharov, V. S., Ferrington, D. A., Squier, T. C. and Schöneich, C. (1999) Diastereoselective  
588 reduction of protein-bound methionine sulfoxide by methionine sulfoxide reductase. *FEBS*  
589 *Lett.* **455**, 247–250.
- 590 8 Vogt, W. (1995) Oxidation of methionyl residues in proteins: tools, targets, and reversal. *Free*  
591 *Radic. Biol. Med.* **18**, 93–105.
- 592 9 Ejiri, S. I., Weissbach, H. and Brot, N. (1979) Reduction of methionine sulfoxide to  
593 methionine by *Escherichia coli*. *J. Bacteriol.* **139**, 161–164.
- 594 10 Lowther, W. T., Weissbach, H., Etienne, F., Brot, N. and Matthews, B. W. (2002) The  
595 mirrored methionine sulfoxide reductases of *Neisseria gonorrhoeae* pilB. *Nat. Struct. Biol.* **9**,  
596 348–352.
- 597 11 Moskovitz, J., Singh, V. K., Requena, J., Wilkinson, B. J., Jayaswal, R. K. and Stadtman, E.  
598 R. (2002) Purification and characterization of methionine sulfoxide reductases from mouse  
599 and *Staphylococcus aureus* and their substrate stereospecificity. *Biochem. Biophys. Res.*  
600 *Commun.* **290**, 62–65.
- 601 12 Vieira Dos Santos, C., Cuiñé, S., Rouhier, N. and Rey, P. (2005) The Arabidopsis plastidic  
602 methionine sulfoxide reductase B proteins. Sequence and activity characteristics, comparison  
603 of the expression with plastidic methionine sulfoxide reductase A, and induction by  
604 photooxidative stress. *Plant Physiol.* **138**, 909–922.
- 605 13 Grimaud, R., Ezraty, B., Mitchell, J. K., Lafitte, D., Briand, C., Derrick, P. J. and Barras, F.  
606 (2001) Repair of oxidized proteins. Identification of a new methionine sulfoxide reductase. *J.*  
607 *Biol. Chem.* **276**, 48915–48920.
- 608 14 Kumar, R. A., Koc, A., Cerny, R. L. and Gladyshev, V. N. (2002) Reaction mechanism,  
609 evolutionary analysis, and role of zinc in *Drosophila* methionine-R-sulfoxide reductase. *J.*  
610 *Biol. Chem.* **277**, 37527–37535.
- 611 15 Tarrago, L., Kaya, A., Weerapana, E., Marino, S. M. and Gladyshev, V. N. (2012)  
612 Methionine sulfoxide reductases preferentially reduce unfolded oxidized proteins and protect  
613 cells from oxidative protein unfolding. *J. Biol. Chem.* **287**, 24448–24459.
- 614 16 Tarrago, L. and Gladyshev, V. N. (2012) Recharging oxidative protein repair: catalysis by  
615 methionine sulfoxide reductases towards their amino acid, protein, and model substrates.  
616 *Biochem. Biokhimiia* **77**, 1097–1107.

- 617 17 Kim, H.-Y. (2013) The methionine sulfoxide reduction system: selenium utilization and  
618 methionine sulfoxide reductase enzymes and their functions. *Antioxid. Redox Signal.* **19**,  
619 958–969.
- 620 18 Châtelain, E., Satour, P., Laugier, E., Ly Vu, B., Payet, N., Rey, P. and Montrichard, F.  
621 (2013) Evidence for participation of the methionine sulfoxide reductase repair system in plant  
622 seed longevity. *Proc. Natl. Acad. Sci. U. S. A.* **110**, 3633–3638.
- 623 19 Laugier, E., Tarrago, L., Vieira Dos Santos, C., Eymery, F., Havaux, M. and Rey, P. (2010)  
624 *Arabidopsis thaliana* plastidial methionine sulfoxide reductases B, MSRBs, account for most  
625 leaf peptide MSR activity and are essential for growth under environmental constraints  
626 through a role in the preservation of photosystem antennae. *Plant J. Cell Mol. Biol.* **61**, 271–  
627 282.
- 628 20 Saleh, M., Bartual, S. G., Abdullah, M. R., Jensch, I., Asmat, T. M., Petruschka, L., Pribyl,  
629 T., Gellert, M., Lillig, C. H., Antelmann, H., et al. (2013) Molecular architecture of  
630 *Streptococcus pneumoniae* surface thioredoxin-fold lipoproteins crucial for extracellular  
631 oxidative stress resistance and maintenance of virulence. *EMBO Mol. Med.* **5**, 1852–1870.
- 632 21 Skaar, E. P., Tobiason, D. M., Quick, J., Judd, R. C., Weissbach, H., Etienne, F., Brot, N. and  
633 Seifert, H. S. (2002) The outer membrane localization of the *Neisseria gonorrhoeae* MsrA/B  
634 is involved in survival against reactive oxygen species. *Proc. Natl. Acad. Sci. U. S. A.* **99**,  
635 10108–10113.
- 636 22 Le, D. T., Lee, B. C., Marino, S. M., Zhang, Y., Fomenko, D. E., Kaya, A., Hacıoglu, E.,  
637 Kwak, G.-H., Koc, A., Kim, H.-Y., et al. (2009) Functional analysis of free methionine-R-  
638 sulfoxide reductase from *Saccharomyces cerevisiae*. *J. Biol. Chem.* **284**, 4354–4364.
- 639 23 Lin, Z., Johnson, L. C., Weissbach, H., Brot, N., Lively, M. O. and Lowther, W. T. (2007)  
640 Free methionine-(R)-sulfoxide reductase from *Escherichia coli* reveals a new GAF domain  
641 function. *Proc. Natl. Acad. Sci. U. S. A.* **104**, 9597–9602.
- 642 24 Ezraty, B., Bos, J., Barras, F. and Aussel, L. (2005) Methionine sulfoxide reduction and  
643 assimilation in *Escherichia coli*: new role for the biotin sulfoxide reductase BisC. *J. Bacteriol.*  
644 **187**, 231–237.
- 645 25 Dhoub, R., Othman, D. S. M. P., Lin, V., Lai, X. J., Wijesinghe, H. G. S., Essilfie, A.-T.,  
646 Davis, A., Nasreen, M., Bernhardt, P. V., Hansbro, P. M., et al. (2016) A Novel,  
647 Molybdenum-Containing Methionine Sulfoxide Reductase Supports Survival of  
648 *Haemophilus influenzae* in an In vivo Model of Infection. *Front. Microbiol.* **7**, 1743.
- 649 26 Weiner, J. H., MacIsaac, D. P., Bishop, R. E. and Bilous, P. T. (1988) Purification and  
650 properties of *Escherichia coli* dimethyl sulfoxide reductase, an iron-sulfur molybdoenzyme  
651 with broad substrate specificity. *J. Bacteriol.* **170**, 1505–1510.
- 652 27 Abo, M., Tachibana, M., Okubo, A. and Yamazaki, S. (1995) Enantioselective deoxygenation  
653 of alkyl aryl sulfoxides by DMSO reductase from *Rhodobacter sphaeroides* f.s. *denitrificans*.  
654 *Bioorg. Med. Chem.* **3**, 109–112.
- 655 28 Gennaris, A., Ezraty, B., Henry, C., Agrebi, R., Vergnes, A., Oheix, E., Bos, J., Leverrier, P.,  
656 Espinosa, L., Szewczyk, J., et al. (2015) Repairing oxidized proteins in the bacterial envelope  
657 using respiratory chain electrons. *Nature* **528**, 409–412.
- 658 29 Melnyk, R. A., Youngblut, M. D., Clark, I. C., Carlson, H. K., Wetmore, K. M., Price, M. N.,  
659 Iavarone, A. T., Deutschbauer, A. M., Arkin, A. P. and Coates, J. D. (2015) Novel  
660 mechanism for scavenging of hypochlorite involving a periplasmic methionine-rich Peptide  
661 and methionine sulfoxide reductase. *mBio* **6**, e00233-00215.
- 662 30 Juillan-Binard, C., Picciocchi, A., Andrieu, J.-P., Dupuy, J., Petit-Hartlein, I., Caux-Thang,  
663 C., Vivès, C., Nivière, V. and Fieschi, F. (2016) A two-component NOX-like system in

- 664 bacteria is involved in the electron transfer chain to the methionine sulfoxide reductase MsrP.  
665 J. Biol. Chem.
- 666 31 Glaeser, J., Zobawa, M., Lottspeich, F. and Klug, G. (2007) Protein synthesis patterns reveal  
667 a complex regulatory response to singlet oxygen in *Rhodobacter*. J. Proteome Res. **6**, 2460–  
668 2471.
- 669 32 Sabaty, M., Grosse, S., Adryanczyk, G., Boiry, S., Biaso, F., Arnoux, P. and Pignol, D.  
670 (2013) Detrimental effect of the 6 His C-terminal tag on YedY enzymatic activity and  
671 influence of the TAT signal sequence on YedY synthesis. BMC Biochem. **14**, 28.
- 672 33 Prentki, P. and Krisch, H. M. (1984) In vitro insertional mutagenesis with a selectable DNA  
673 fragment. Gene **29**, 303–313.
- 674 34 Quandt, J. and Hynes, M. F. (1993) Versatile suicide vectors which allow direct selection for  
675 gene replacement in gram-negative bacteria. Gene **127**, 15–21.
- 676 35 Hartmann, E. M., Allain, F., Gaillard, J.-C., Pible, O. and Armengaud, J. (2014) Taking the  
677 shortcut for high-throughput shotgun proteomic analysis of bacteria. Methods Mol. Biol.  
678 Clifton NJ **1197**, 275–285.
- 679 36 Madeira, J.-P., Alpha-Bazin, B. M., Armengaud, J. and Duport, C. (2017) Methionine  
680 Residues in Exoproteins and Their Recycling by Methionine Sulfoxide Reductase AB Serve  
681 as an Antioxidant Strategy in *Bacillus cereus*. Front. Microbiol. **8**, 1342.
- 682 37 Klein, G., Mathé, C., Biola-Clier, M., Devineau, S., Drouineau, E., Hatem, E., Marichal, L.,  
683 Alonso, B., Gaillard, J.-C., Lagniel, G., et al. (2016) RNA-binding proteins are a major target  
684 of silica nanoparticles in cell extracts. Nanotoxicology **10**, 1555–1564.
- 685 38 Colaert, N., Helsens, K., Martens, L., Vandekerckhove, J. and Gevaert, K. (2009) Improved  
686 visualization of protein consensus sequences by iceLogo. Nat. Methods **6**, 786–787.
- 687 39 Kim, Y. K., Shin, Y. J., Lee, W.-H., Kim, H.-Y. and Hwang, K. Y. (2009) Structural and  
688 kinetic analysis of an MsrA-MsrB fusion protein from *Streptococcus pneumoniae*. Mol.  
689 Microbiol. **72**, 699–709.
- 690 40 Ray, S. S., Singh, S. K. and Balaram, P. (2001) An electrospray ionization mass spectrometry  
691 investigation of 1-anilino-8-naphthalene-sulfonate (ANS) binding to proteins. J. Am. Soc.  
692 Mass Spectrom. **12**, 428–438.
- 693 41 Ghesquière, B., Jonckheere, V., Colaert, N., Van Durme, J., Timmerman, E., Goethals, M.,  
694 Schymkowitz, J., Rousseau, F., Vandekerckhove, J. and Gevaert, K. (2011) Redox  
695 proteomics of protein-bound methionine oxidation. Mol. Cell. Proteomics MCP **10**,  
696 M110.006866.
- 697 42 Hsieh, Y.-J., Chien, K.-Y., Yang, I.-F., Lee, I.-N., Wu, C.-C., Huang, T.-Y. and Yu, J.-S.  
698 (2017) Oxidation of protein-bound methionine in Photofrin-photodynamic therapy-treated  
699 human tumor cells explored by methionine-containing peptide enrichment and quantitative  
700 proteomics approach. Sci. Rep. **7**, 1370.
- 701 43 Jacques, S., Ghesquière, B., De Bock, P.-J., Demol, H., Wahni, K., Willems, P., Messens, J.,  
702 Van Breusegem, F. and Gevaert, K. (2015) Protein Methionine Sulfoxide Dynamics in  
703 *Arabidopsis thaliana* under Oxidative Stress. Mol. Cell. Proteomics MCP **14**, 1217–1229.
- 704 44 Luo, S. and Levine, R. L. (2009) Methionine in proteins defends against oxidative stress.  
705 FASEB J. Off. Publ. Fed. Am. Soc. Exp. Biol. **23**, 464–472.
- 706 45 Winter, J., Ilbert, M., Graf, P. C. F., Ozcelik, D. and Jakob, U. (2008) Bleach activates a  
707 redox-regulated chaperone by oxidative protein unfolding. Cell **135**, 691–701.
- 708 46 Loschi, L., Brokx, S. J., Hills, T. L., Zhang, G., Bertero, M. G., Lovering, A. L., Weiner, J.  
709 H. and Strynadka, N. C. J. (2004) Structural and Biochemical Identification of a Novel  
710 Bacterial Oxidoreductase. J. Biol. Chem. **279**, 50391–50400.

711 **Table**

712 **Table 1.** Kinetics parameters of RsMsrP reductase activity towards DMSO and various MetO-containing  
713 substrates.

<b>Substrates</b>	<b><math>k_{\text{cat}}</math> (<math>\text{s}^{-1}</math>)</b>	<b><math>K_{\text{m}}</math></b> <b>(<math>\mu\text{M}</math>)</b>	<b><math>k_{\text{cat}}/K_{\text{m}}</math></b> <b>(<math>\text{M}^{-1}.\text{s}^{-1}</math>)</b>
DMSO <sup>a</sup>	$28 \pm 1$	$61,000 \pm 7,000$	465
Free L-Met- <i>R,S</i> -O	$122 \pm 20$	$115,000 \pm 27,000$	1,000
Ser-MetO-Ser	$108 \pm 17$	$13,000 \pm 3,400$	8,300
QWGAGM(O)QAEED	$479 \pm 24$	$4,530 \pm 370$	105,700
TTPGYM(O)EEWNK	> 70	> 5,000	N.D.
Oxidized $\beta$ -casein	$100 \pm 5$	$93 \pm 9$	1,075,000
$\beta$ -casein- <i>R</i> -O	$49 \pm 3$	$51 \pm 6$	950,000
$\beta$ -casein- <i>S</i> -O	$8 \pm 1$	$53 \pm 10$	142,000
Oxidized lysozyme	$4 \pm 1$	$886 \pm 349$	4,000
Unfolded oxidized lysozyme	$7 \pm 1$	$105 \pm 17$	70,200
Oxidized GST	$8 \pm 2$	$643 \pm 194$	12,400
Unfolded oxidized GST	$12 \pm 3$	$99 \pm 33$	120,000

714 <sup>a</sup> From [32]. *N.D.*, not determined.

715

716 **Figures legends**

717 **Figure 1. Mass spectrometry spectrum of  $\beta$ -casein non-oxidized (A), oxidized with  $H_2O_2$  (B) and**

718 **repaired by RsMsrP (C).** A) Commercial  $\beta$ -casein exists as a mixture of genetic variants (7 in our batch).

719  $\beta$ -casein was analyzed by ESI-MS. Main peaks masses: 1, 23982.7 Da; 2, 24021.6 Da; 3, 24035.9 Da; 4,

720 24075.0 Da; 5, 24089.1 Da; 6, 24127.5 Da; 7, 24142.5 Da. B)  $\beta$ -casein was oxidized with 50 mM  $H_2O_2$

721 before MS analysis. All major peaks underwent an increase of  $\sim 96$  Da compared to the non-oxidized

722 sample. Main peaks masses: 1, 24079.1 Da; 2, 24118.5 Da; 3, 24131.8 Da; 4, 24172.2 Da; 5, 24184.3 Da;

723 6, 24224.4 Da; 7, 24238.2 Da. C) Oxidized  $\beta$ -casein was incubated with RsMsrP (25 nM) in the presence

724 of BV (0.8 mM) and sodium dithionite (2 mM) as electron donors. All major peaks had masses

725 corresponding of the non-oxidized  $\beta$ -casein, showing the ability to reduce all MetO in this protein. Note the

726 presence of a peak with an increase of 16 Da (\*, mass of 23999.4 Da) compared to the main reduced peak,

727 indicating an incomplete reduction of the total protein pool. Main peaks masses: 1, 23983.0 Da; 2, 24022.4

728 Da; 3, 24037.1 Da; 4, 24075.0 Da; 5, 24091.0 Da; 6, 24128.2 Da; 7, 24143.7 Da.

729 **Figure 2. RsMsrP activity using oxidized  $\beta$ -casein,  $\beta$ -casein-*R-O* and  $\beta$ -casein-*S-O* as substrates.** The

730 oxidized  $\beta$ -casein (100  $\mu$ M) containing both diastereomers of MetO, only the *R* one (" *$\beta$ -casein-*R-O**"), or

731 only the *S* one (" *$\beta$ -casein-*S-O**") were assayed as substrates of RsMsrP. The RsMsrP activity was determined

732 using benzyl viologen (BV) (0.8 mM) as an electron provider in a glove box under nitrogen. BV was initially

733 reduced with sodium dithionite (2 mM) and oxidation was followed at 600 nm after addition of the enzyme

734 (30 nM). The reaction was done in 50 mM MES, pH6.0. The activity values presented as  $k_{cat}$  ( $s^{-1}$ ) represent

735 the number of mole of MetO reduced per mole of enzyme per second as 2 moles of BV is oxidized per mole

736 of MetO reduced. Data presented are averages of 3 replicates.  $\pm$  S.D.

737 **Figure 3. Characteristics of MetO reduction sites and oxidation state of Met in representative**

738 **proteins.** A) Repartition of the number of MetO per percentage of reduction by RsMsrP. B) Percentage of

739 oxidation of Met 353 of putative ABC transporter from HAAT family in the 3 analyzed samples. C)

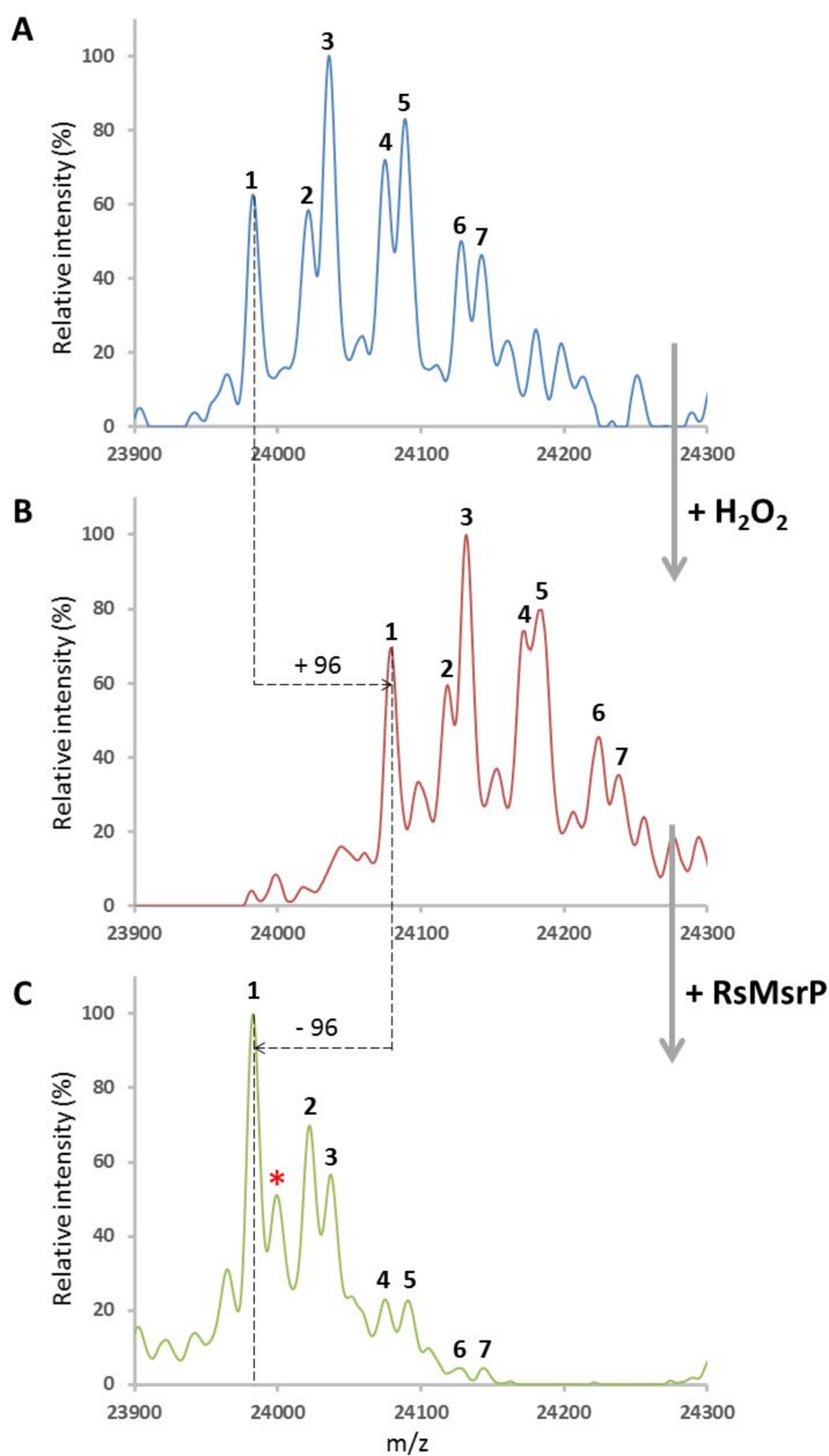
740 Percentage of oxidation of Met 230 and 243 of ABC transporter DdpA. D) Percentage of oxidation of Met

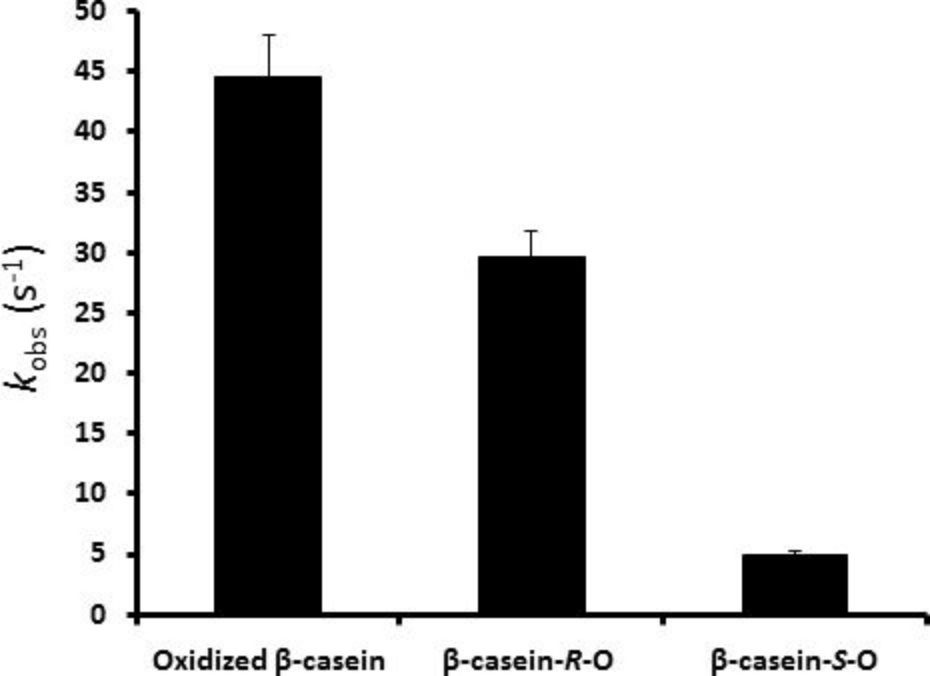
741 92, 172 and 190 in the peptidyl-prolyl cis-trans isomerase. E) Percentage of oxidation of Met 123, 438 and  
742 539 of the pyrroloquinoline quinone (PQQ) dehydrogenase XoxF.

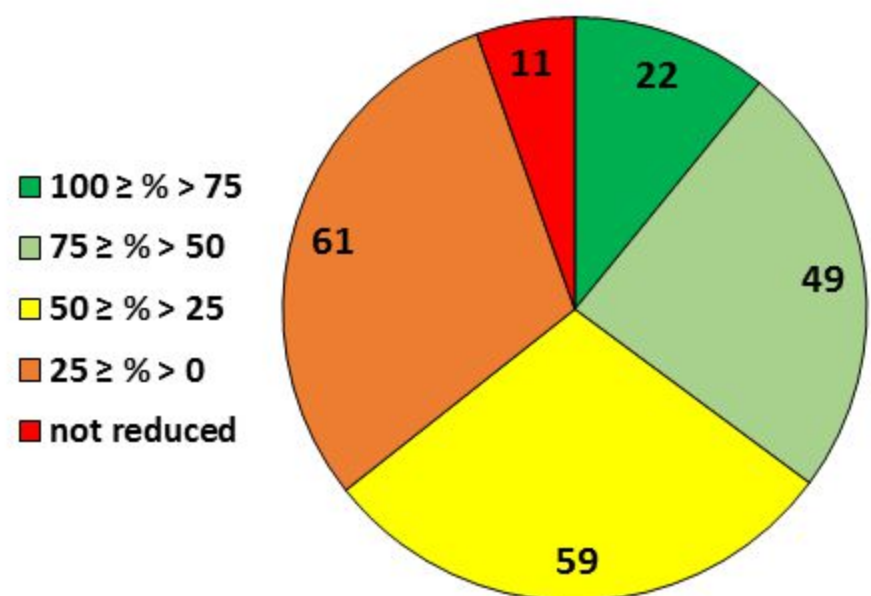
743 **Figure 4. IceLogo representation of enriched and depleted amino acids around the sites of Met**  
744 **oxidation.** A) Enrichment and depletion of amino acids around the oxidized Met (M) found in periplasmic  
745 extracts and oxidized periplasmic extracts by comparison with the theoretical proteome of *R. sphaeroides*.  
746 B) The same oxidized peptides were analyzed using the peptides containing a non-oxidized Met from the  
747 same samples (periplasm and oxidized periplasm extracts). Amino acids are colored according to their  
748 physiochemical properties.

749 **Figure 5. IceLogo representation of enriched and depleted amino acids around the sites of MetO**  
750 **reduction by RsMsP.** A) Enrichment of amino acids in peptides centered on the MetO for which the  
751 percentage of reduction and the decrease in the percentage of oxidation were both superior to 50 % by  
752 comparison with the theoretical proteome of *R. sphaeroides*. B) Enrichment of amino acids from peptides  
753 centered on the MetO for which the percentage of reduction and the decrease in percentage were inferior to  
754 10 % by comparison with the theoretical proteome of *R. sphaeroides*. C) Enrichment and depletion of amino  
755 acids from efficiently reduced MetO-containing peptides (dataset used in A)) by comparison with  
756 inefficiently reduced MetO-containing peptides (dataset used in B)). Amino acids are colored according to  
757 their physiochemical properties.

758 **Figure 6. Relative RsMsP activity using unfolded oxidized proteins.** The RsMsP activity was  
759 determined as described in Figure 2. Oxidized and unfolded oxidized lysozyme were incubated at 100  $\mu\text{M}$   
760 in 50 mM MES, pH 6.0. Initial turnover numbers were  $0.65 \pm 0.12 \text{ s}^{-1}$  and  $7.38 \pm 0.23 \text{ s}^{-1}$  with oxidized and  
761 unfolded oxidized lysozyme, respectively. Activity with oxidized and unfolded oxidized GST (75  $\mu\text{M}$ ) was  
762 determined similarly except that reaction buffer was 30 mM Tris-HCl, pH 8.0 because unfolded oxidized  
763 GST precipitated in 50 mM MES, pH 6.0. Initial turnover numbers were  $0.86 \pm 0.08 \text{ s}^{-1}$  and  $5.31 \pm 0.39 \text{ s}^{-1}$   
764 with oxidized and unfolded oxidized GST, respectively. Data presented are averages of three replicates.  $\pm$   
765 S.D.

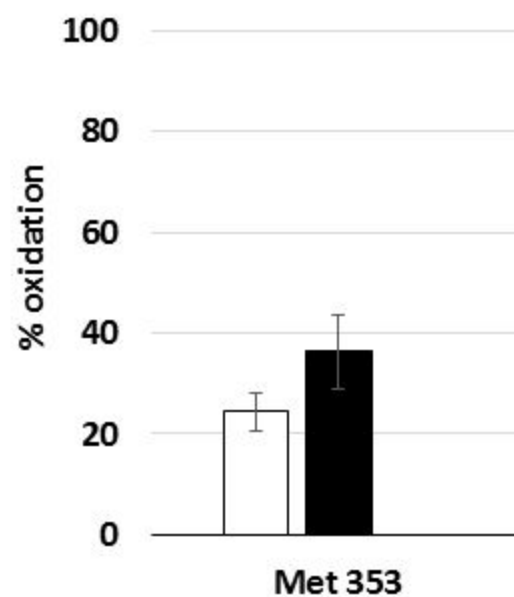




**A****B**

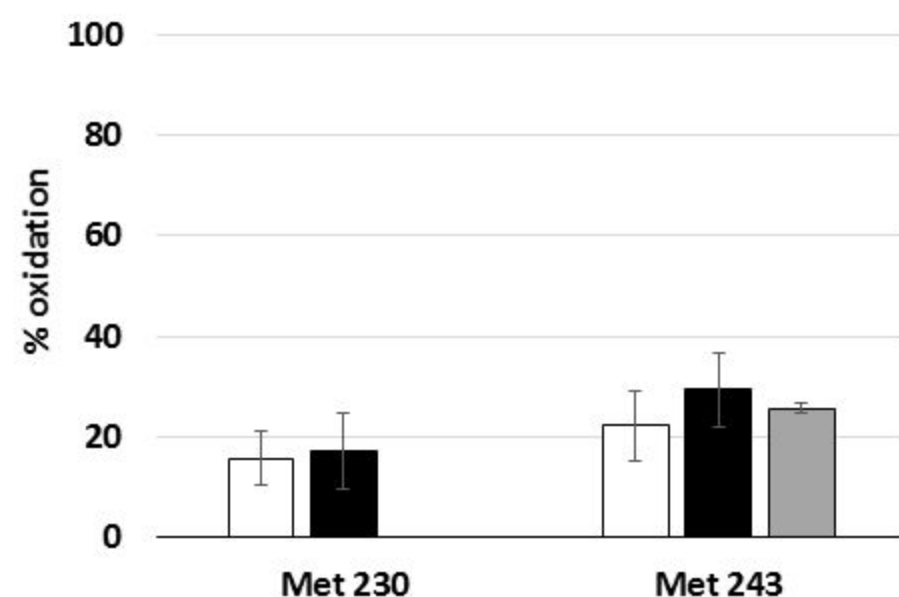
ABC trans. HAAT-fam.

□ Peri. ■ Ox. Peri. ■ Rep. ox. peri.

**C**

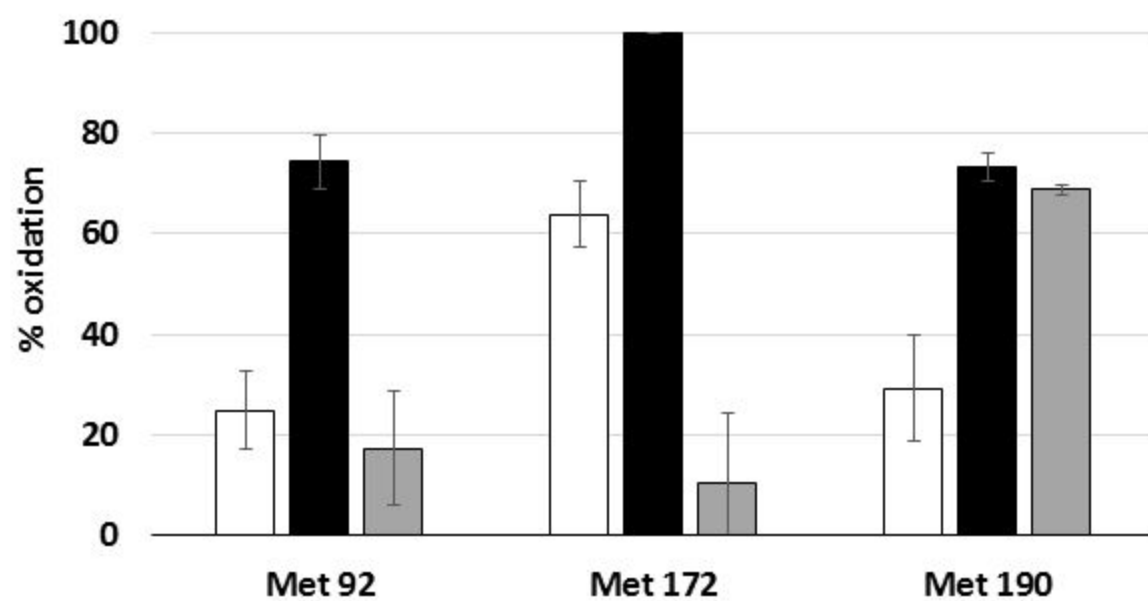
ABC transporter DdpA

□ Peri. ■ Ox. Peri. ■ Rep. ox. peri.

**D**

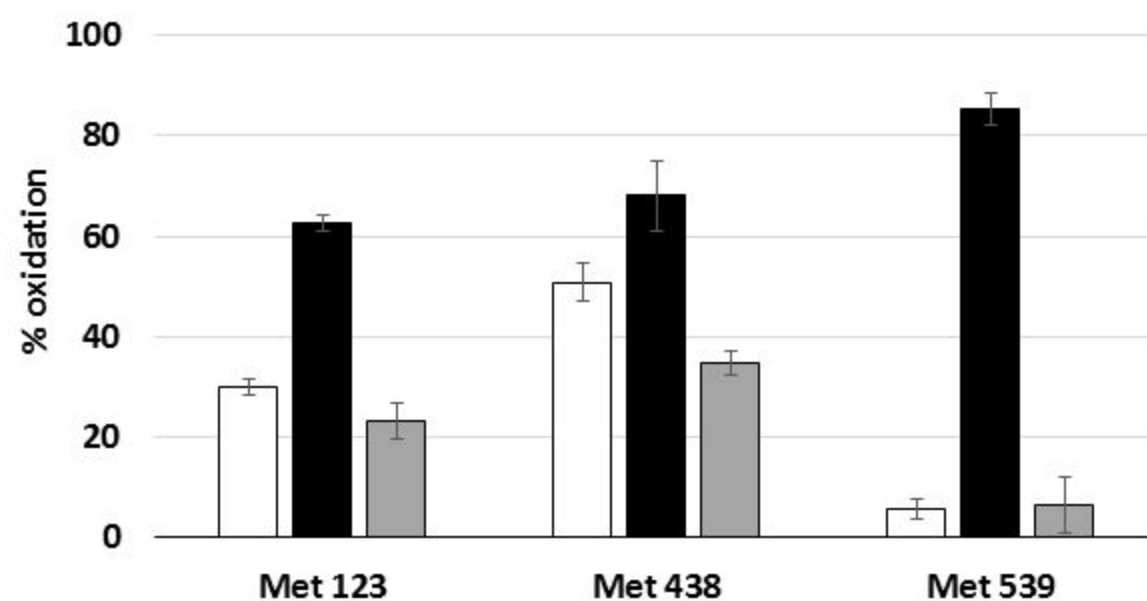
Peptidyl-prolyl cis-trans isomerase

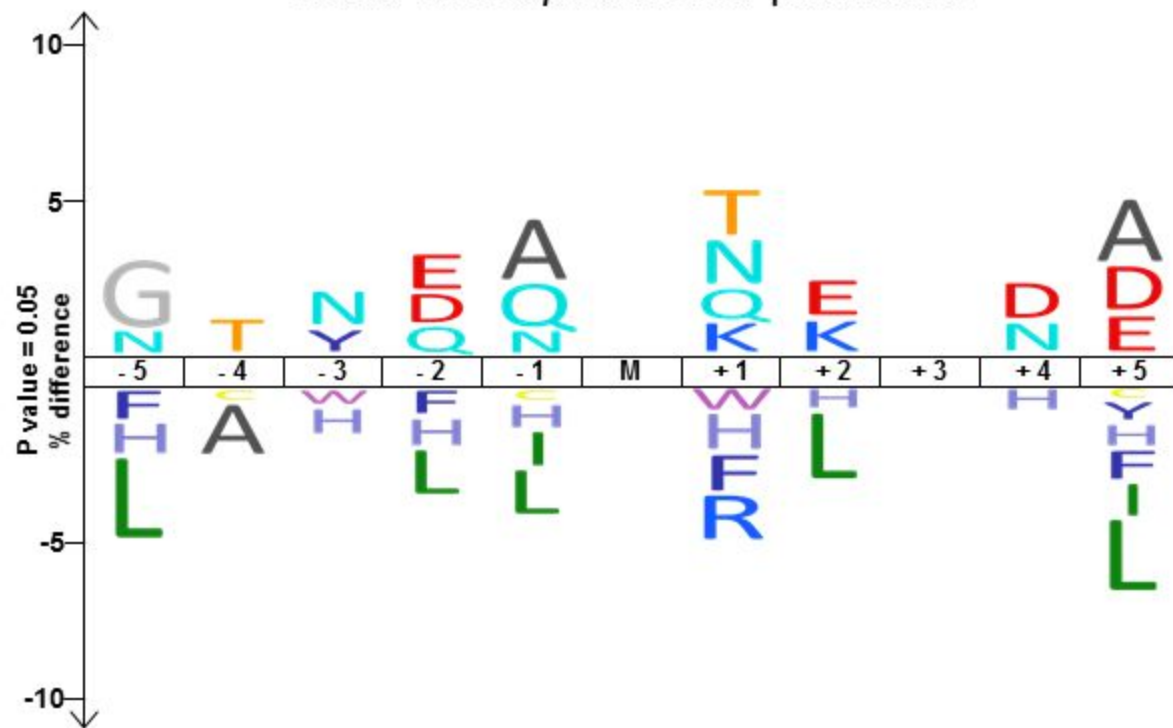
□ Peri. ■ Ox. Peri. ■ Rep. ox. peri.

**E**

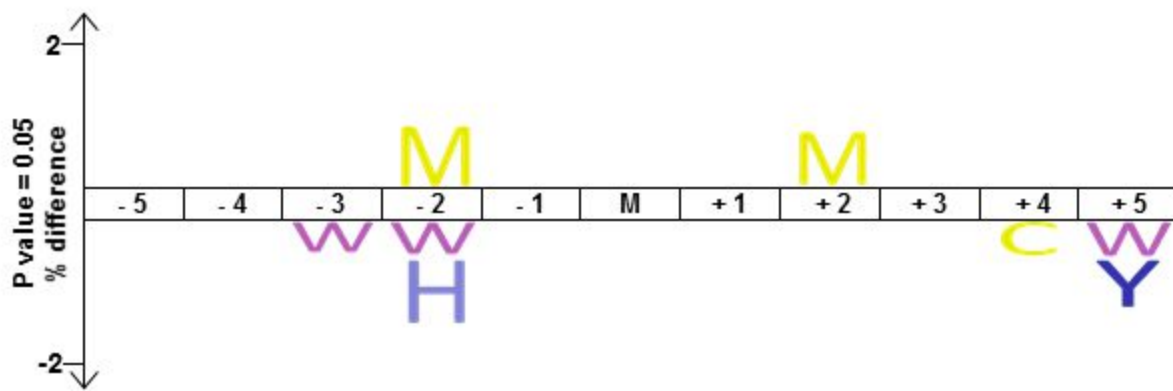
PQQ dehydrogenase XoxF

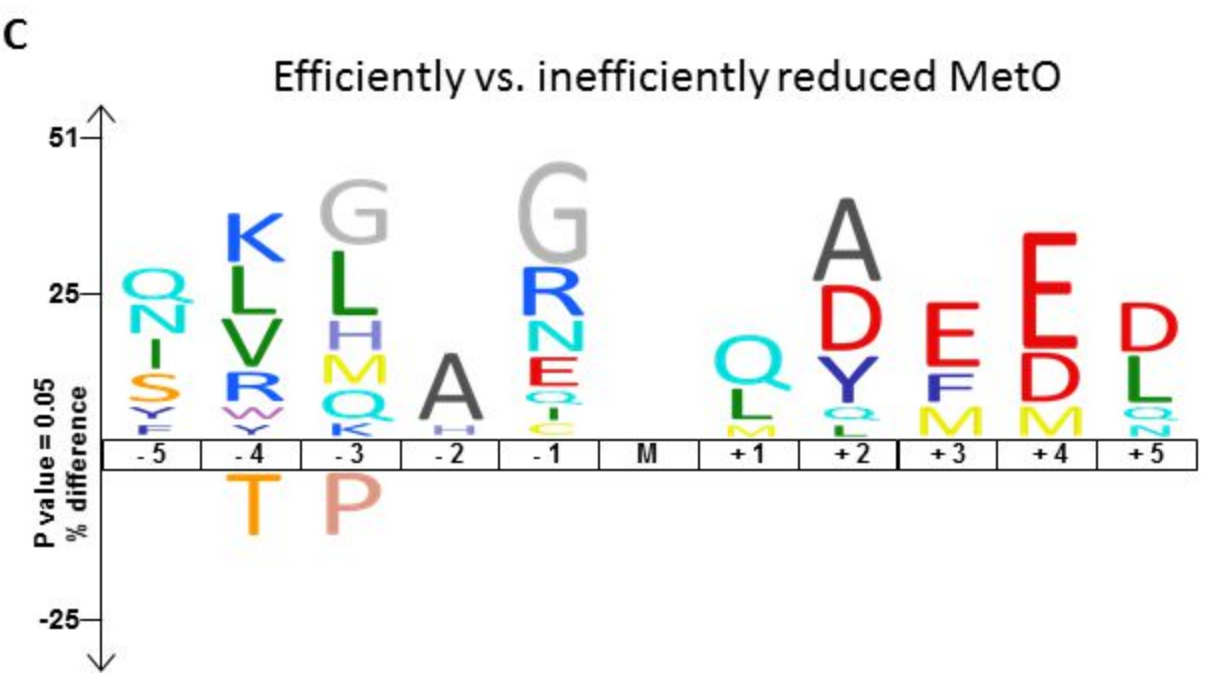
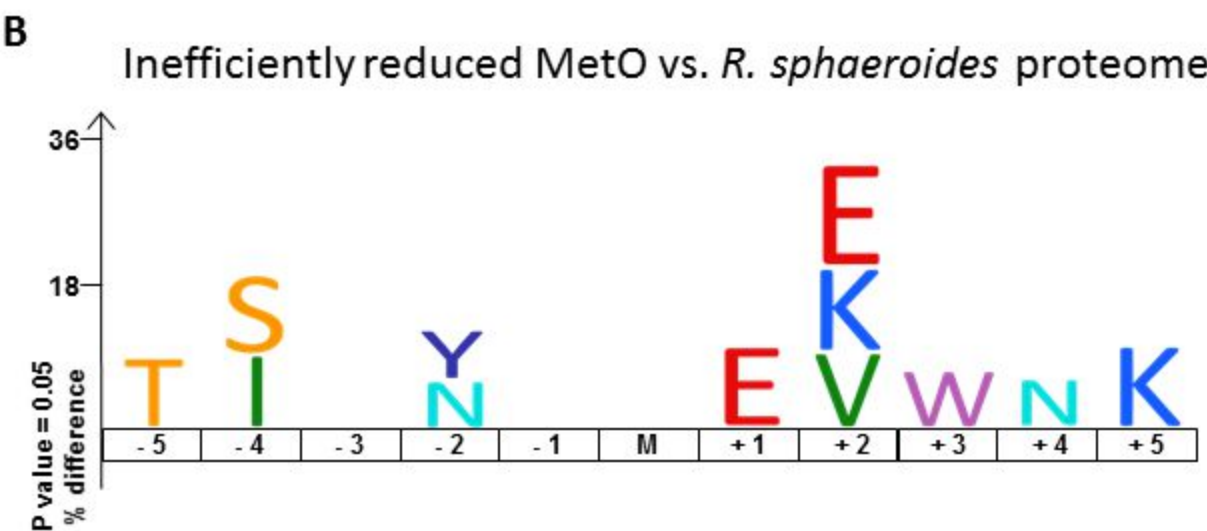
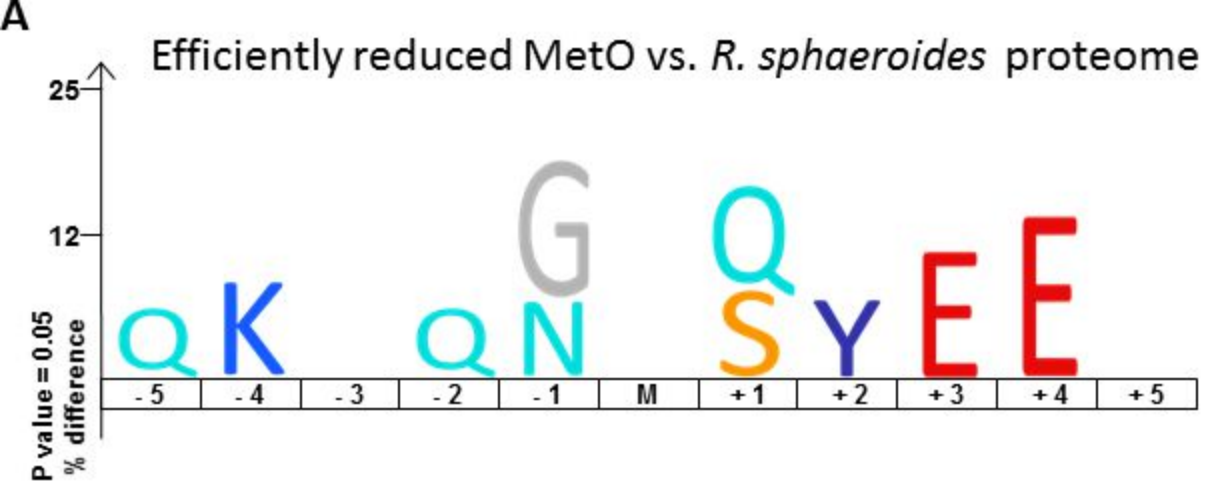
□ Peri. ■ Ox. Peri. ■ Rep. ox. peri.



**A**MetO vs. *R. sphaeroides* proteome**B**

## MetO vs. Met





Relative RsMSRP activity

